Graphical Presentation Chapter IV

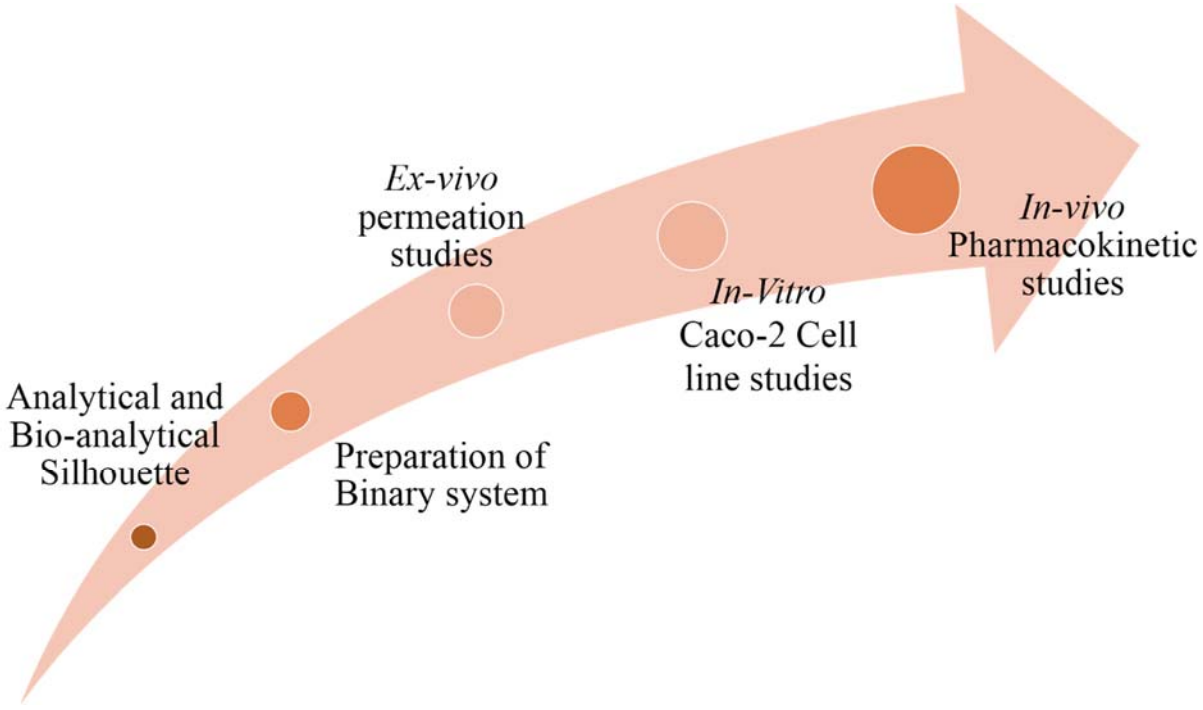

4.0. Introduction

Acyclovir (ACV), was the first and potent molecule for the treatment of herpes simplex virus. It is the most important and widely used drug for anti-viral therapy. According to a survey in the United States it has been concluded that more than 50% adults suffer from the herpes infection. In this scenario the ACV is the most prescribed drug for the treatment of infection (1). In the literature, it has been clearly mentioned that ACV (BCS Class III Drug) has several issues with its oral bioavailability (2) also including the variability in the bioavailability has been reported. Despite of this it also has some sever systemic toxicity effects. To improve the therapy of the ACV several approaches in the past has been tried out, such as formulating ACV in matrix tablets (3), microspheres (4) and polymeric films (5). Although, they either needed some sophisticated procedures and some are not that much safer due to adverse drug reactions. In this research work we are introducing a novel concept of combination with the natural bioenhancers (6, 7). As the name suggests natural, they are safer as compare to other combination therapies and also act as drug facilitators for permeation through the gut wall. The bioenhancers incorporated with the ACV are Quercetin (QU), Silibinin (Sil) and Luteolin (LT).

In this chapter, study of the effect of natural bioenhancers on the oral uptake of acyclovir (ACV) has been described with all the experimental protocols summed with a conclusion. The present investigation was enthused by the prospect of the combination of natural bioenhancer with the ACV and to evaluate their effect on the oral uptake of the ACV. In the proposed work ACV:QU, ACV:Sil and ACV:LT binary mixtures were prepared using different weight ratios of ACV with the help of physical mixing method. The prepared binary mixtures were studied for compatibility using FTIR and DSC. Oral uptake was

studied by analyzing the transport of ACV across the human colorectal adenocarcinoma cell line (Caco-2) cell lines. Permeation through the goat intestine tissue was also studied. Pharmacokinetic analysis was also performed in rabbits by administered ACV with different bioenhancers in the form of suspension, and the whole analytical studies for the estimation of ACV in different studies were conducted using LC-MS. In the compatibility studies, bioenhancers found to be showing no or minimal interaction with the ACV. Permeation in the intestinal tissue of goat was significantly increased as compared to the plain drug. The transport of ACV across the Caco-2 cell lines also found to be improved than the plain drug. Pharmacokinetic study showed there was increase in the Cmax using the different bioenhancers. AUC was also found to be increase with the each bioenahncer. The maximum oral uptake enhancement was found with the QU following by the Sil and then LT. This increase uptake here by increasing the bioavailability as well as increasing the therapy efficiency.

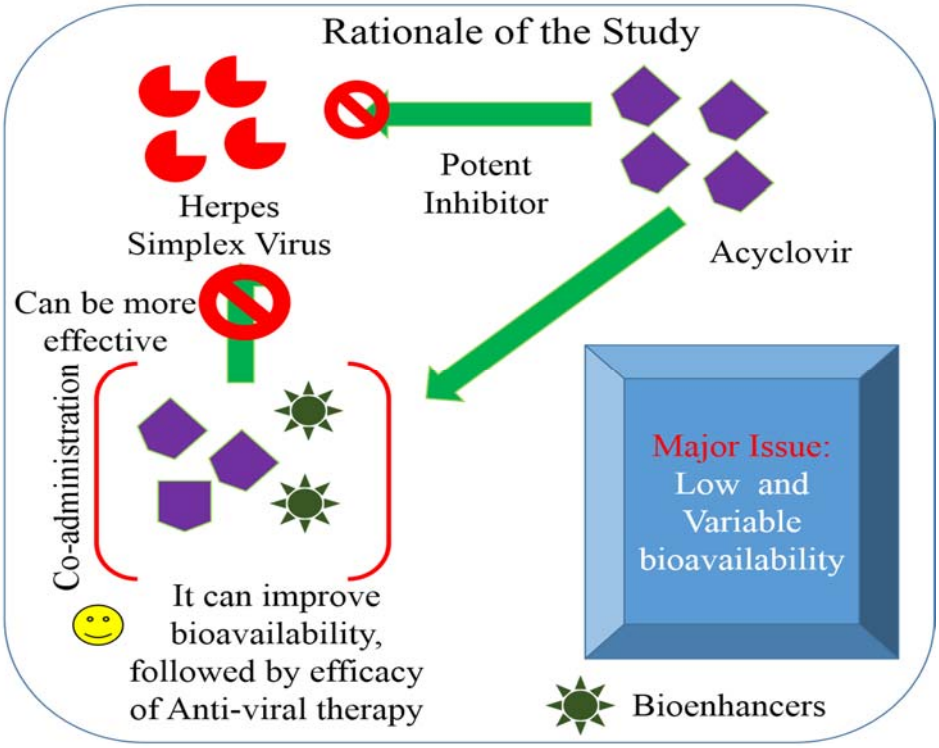

4.1. Material and Methods

4.1.1. Materials and reagents

Acyclovir was procured as gift sample from Nestor Pharmaceutical Pvt. Ltd., India. Various commercial formulations of acyclovir were purchased from local drug store. Quercetin, Silibinin and Luteolin was purchased from Sigma-Aldrich. Caco-2 cell lines were obtained from NCCS Pune. All the reagents used in this study were of analytical grade and were commercially procured.

4.1.2. Analytical and Bio-analytical Method development and Validation

4.1.2.1. Zero order UV Spectroscopy method

4.1.2.1.1. Instrumentation

Spectrophotometric measurements were made on a Shimadzu 1700 double beam UV–VIS spectrophotometer with a fix slit width of 1 nm coupled with Shimadzu UV PC software (UV probe) version 2.31. Weighing balance of Shimadzu AX120, bath sonicator (Electroquip) and borosil glass apparatus were used for experimental purpose.

4.1.2.1.2. Preparation of standard solutions

An accurately weighed amount of ACV was transferred into a 10 mL calibrated flask and dissolved in approximately 4 mL of 0.1M HCl. The resulting solutions were completed to the mark with 0.1M HCl obtaining stock standard solution containing 1000 µg/mL. Different volumes of this stock solution were then further diluted with 0.1M HCl to obtain the working standard solutions.

4.1.2.1.3. Sample preparation

4.1.2.1.3.1. Tablets

Twenty tablets were finely powdered and an accurately weighed quantity of the powdered tablets content equivalent to 10 mg of the active ingredient was transferred into a 10 mL calibrated flask and dissolved in about 6 mL of 0.1M HCl. The contents of the flask were swirled, sonicated up to 9 min and then volume of the flask was made up with 0.1M HCl. The content were mixed well, filtered and the first portion of the filtrate was rejected. The prepared solution was diluted quantitatively with the 0.1M HCl to obtain a suitable concentration for analysis.

4.1.2.1.3.2. Cream samples

An accurately weighed amount of the cream equivalent to 10 mg of ACV was shaken with 5 mL of 0.1M HCl and sonicated for 15 min and then the volume was made up to the mark with 0.1M HCl. The resulting solution was filtered and first portion of the filtrate was discarded. The working solutions were prepared by further diluting with 0.1M HCl for analysis.

4.1.2.1.3.3. Eye ointment sample

Eye ointment equivalent to 10 mg of ACV was dispersed in few mL of 0.1M HCl, sonicated for 18 min and the volume was made up with 0.1M HCl. The resulting solution was filtered, and first portion of the filtrate was rejected. The working solution was prepared by further diluting with 0.1M HCl for analysis.

4.1.2.1.3.4. Injection

To determine the drug in injectable dosage form, the contents per injection were diluted with 0.1M HCl and then sonicated for 9 min and the volume was made up with 0.1M

HCl. The resulting solution was filtered, and first portion of the filtrate was rejected. The working solution was prepared by further diluting with 0.1M HCl for analysis.

4.1.2.1.4. Procedure for spectrophotometric determination

All reagents were tested for stability in solution and during the actual analysis. The behavior of analyte remained unchanged to about 24 h from their preparation at room temperature. The drug was found to be stable during each kind of experimental measurements. Each measurement was done at room temperature. The absorption spectra of the standard solutions were recorded between 200-400 nm against a reagent blank (the same for samples without the analyte to be determined) using a 1.0 cm quartz cell. The zero-order spectrum of pure drug was obtained and absorption maxima was found to be at 257nm.

4.1.2.1.5. Validation parameters studied using total error approach

The present method was validated according to the ICH (8, 9) and the ISO-17025 applying accuracy profiles, which are based upon the "total error" approach (10). This approach estimates the "total error" by combining the systemic error (trueness) and the random error (intermediate precision) to know the difference between the observed result and the true value. In other words, the highest error of an analytical method can be estimated. In the proposed method different parameters such as sensitivity, robustness and assay determination were also studied.

4.1.2.1.5.1. Response function (calibration curve)

In the proposed method four sets of calibration curve were plotted between absorbance and different concentrations of ACV which follows *Lambert's -beer* law and on these four different series regression analysis was performed and series with best coefficient of

determination was selected and the selected linearity has been diagnosed by the Lack of Fit, Levene's test and standard residual plot.

4.1.2.1.5.2. Trueness

According to the ISO, trueness of an analytical procedure expresses the closeness of agreement between the average value obtained from repeated measurements and a conventional true value (11). In this method trueness of calibration curve is calculated to justify the calibration line by back calculating concentrations and results are expressed in terms of absolute and relative bias, and also a linear relationship between introduced and back calculated concentrations has been plotted to demonstrate method linearity.

4.1.2.1.5.3. Precision

The precision of an analytical method expresses the closeness of agreement between the values obtained from repeated measurements. In this method precision at two levels was studied, first one is repeatability under the same operating conditions over a short time interval and second is the intermediate precision assessed on different days. The precision results are expressed using relative standard deviations (RSD). Relative and absolute precision at these two levels were calculated and also 95% upper confidence limit for both levels has been calculated.

4.1.2.1.5.4. Accuracy

Accuracy is the most critical parameter in method validation, so it requires an extra care during the study and taking this in account the results of accuracy studies are represented in the β-expectation tolerance limits. In addition to this, risk profile has also been studied to know the future application of the method in different matrices. Accuracy profiles for the four different matrices have been plotted with β-expectation tolerance limits.

Linearity profile was also studied to demonstrate the relationship between nominal and observed concentration in different matrices and furthermore, residual plot was generated to know the outliers in the determination of ACV in sample matrix.

4.1.2.1.5.5. Limit of detection and quantification

Limit of detection (LOD) and limit of quantification (LOQ) are two important parameters which show the application of method in quantification and detection of different samples. These are calculated according to the procedure mentioned in the ICH guidelines.

4.1.2.1.5.6. Robustness

In daily routine analysis some human or system errors are always there in sample preparation and system measurement properties. A method should be steady to avoid these errors or small variations and should not deviate from its capability of producing reliable results. So, to confirm this robustness studies were performed. Robustness was examined by evaluating the influence of small variation of method variables including solvent grades and detection wavelengths. In these experiments, one parameter was changed whereas the others were kept unchanged and recovery percentage was calculated each time and for all the formulations, recovery experiments for robustness studies were also planned and studied. The robustness studies were conducted with three different wavelengths and three different grades of solvent (HPLC, SD, DD).

Study was conducted by keeping one standard parameter constant and varying second factor respectively.

4.1.2.1.6. Application of proposed method to analysis of dosage forms

After the confirmation of method capacity to analyze ACV, it was subjected to the analysis of different formulation for their contents of ACV. The results for different matrices are calculated in terms of percentage purity. These results confirm the capacity and reliability of the developed method.

4.1.2.1.7. Identification and quantification of different uncertainty parameters

Although the method was validated, still there were some doubts in the results, as few factors were not included in the validation such as errors during mass of sample taken etc. So uncertainty estimation was carried out starting with the identification of sources of uncertainty and compiled up with the CSU and EU results.

4.1.2.1.8. Identification of sources of uncertainty

4.1.2.1.8.1. Construction of the cause and effect diagram

In order to list uncertainty sources, it is very convenient to use the cause and effect diagram because it shows how the sources link to each other and indicate their influence on the result. So a cause and effect diagram was constructed as shown in Figure 4.1, which points out the different sources which may affect the sample analysis measurement. These parameters are: volume of volumetric flask V_{10}, Concentration of analyte C_{10}, mass of sample, Recovery of method R_m and Precision of method. These all parameters contribute to the overall uncertainty in final analytical results in marketed formulations. This diagram will also help in resolving any repeatability of components in uncertainty. These parameters are shown in Eq. 4.1.

$$ACV_{sample} = C_{10}V_{10}10^{-3}/m_{sample}\, R_m \qquad (4.1)$$

Where, ACV_{sample}, ACV quantity (mol/kg); C_{10}, ACV concentration in 10 mL volumetric flask (M); V_{10}, volume of 10 mL volumetric flask (mL); m_{sample}, ACV sample mass taken (kg); Rm, recovery of method.

Now after identification, these sources were quantified and their individual effect on overall uncertainty was studied and compiled up in the form of CSU and EU by carefully choosing coverage factor.

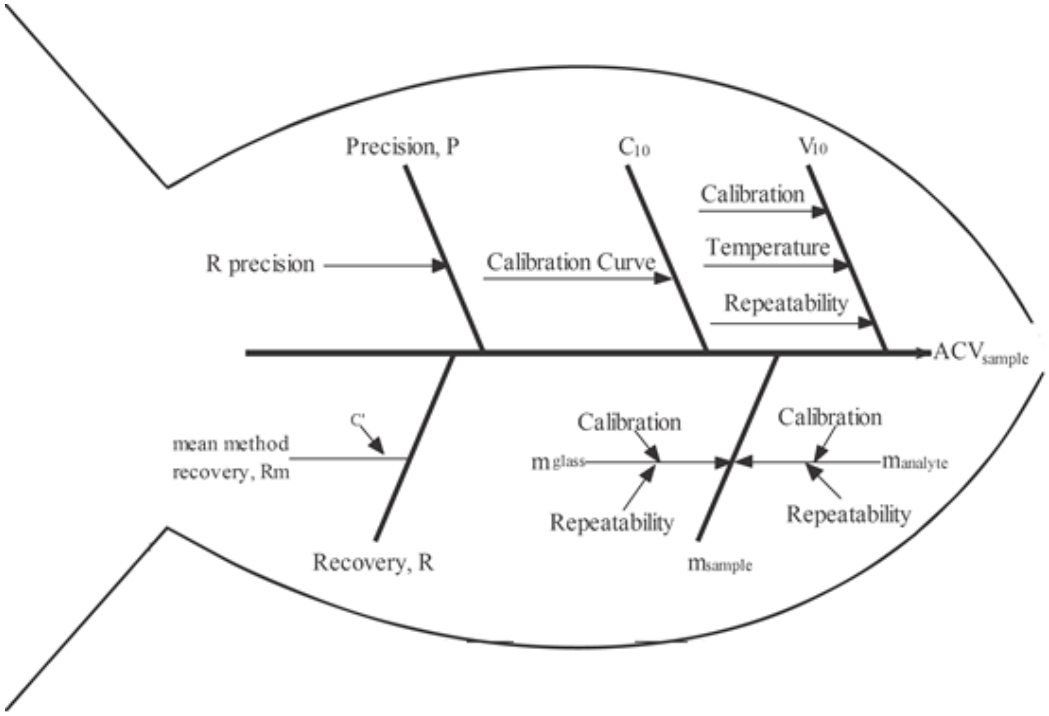

Figure 4.1 Cause and Effect diagram to identify sources for uncertainty

4.1.2.1.9. Individual parameters effecting overall uncertainty

4.1.2.1.9.1. Due to discharge of volumetric flask

The uncertainty due to discharge of volumetric flask was evaluated by performing experiment consisting of filling up and weighing of 10 mL volumetric flask with standard solution repeatedly for ten times.

4.1.2.1.9.2. Due to recovery of method

As the uncertainty associated with the recovery of method depends upon the concentration spiked and recovery observed. So for all the formulations uncertainty associated with recovery of method was evaluated using Eq. 4.3 (11) and recovery was simply calculated by Eq. 4.2.

$$Rm = \frac{Cobs}{Cspike} \qquad (4.2)$$

Where C_{obs}, mean of replicate analysis of spiked sample; C_{spike}, nominal concentration of ACV in spiked sample.

$$U(Rm) = Rm \times \sqrt{\left(\frac{Sobs^2}{n \times Cobs^2}\right) + \left(\frac{U(Cspike)}{Cspike}\right)^2} \qquad (4.3)$$

Where S_{obs}, means standard deviation of results from the replicate analyses of spiked sample; n, number of replicates; $U(C_{spike})$, standard uncertainty in concentration of spiked sample.

4.1.2.1.9.3. Uncertainty due to concentration, C_{10}

The ACV sample concentration uncertainty is expressed as concentration uncertainty from calibration curve and is given by Eq. 4.4.

$$U\,(c) = \frac{Sr}{b}\sqrt{\frac{1}{n} + \frac{1}{p} + \frac{(c - \bar{c})^2}{Sxx}} \qquad (4.4)$$

Where: $S_r = \frac{\sqrt{\sum_{j=1}^{n}[\,Yj - (bxi + a)}}{n-2}$

$$Sxx = \sum(Ci - \bar{c})^2$$

S_r, residual standard deviation; n, number of measurements used for calibration curve; p, number of measurements used to obtain concentration of the sample; c, ACV concentration in sample (M); $\bar{c}$, average of standard solution (M); Y_j, analytical signal of

the measurement; j, index for number of measurements made in order to obtain the calibration curve; i, index for number of solution for calibration; b, slope of calibration curve (L/mol); a, calibration curve intercept;

The sample solution was measured ten times (p = 10) and concentration was obtained from the calibration curve regression equation Eq. 4.5.

$$Y = mx + c \qquad (4.5)$$

Where Y, absorbance of sample; c, calibration curve intercept; m, calibration curve slope; x, concentration of ACV.

4.1.2.1.9.4. Uncertainty due to sample mass m_{sample}

The sample mass was obtained by calculating difference between weighing glass with and without the ACV sample.

4.1.2.1.9.5. Uncertainty due to precision, P

The precision branch collects terms which contribute to random variability of the entire method. Estimate of precision is available from replicate analysis of samples. When the precision studies were carried out and data was obtained, the repeatability and variability associated with that measurement were included in the overall precision uncertainty estimation.

4.1.2.2. LC-MS Method for estimation of ACV in Cell lines and plasma samples

4.1.2.2.1. Instrumentation

Chromatographic study was performed using ekspertTM ultraLC with ekspertTM ultraLC 100 pump system (eksigent-AB Sciex, USA) coupled with 3200 QTRAP mass spectrometer (AB Sciex, USA), located at Dr. Vikram Sarabhai Science Center, Faculty of Science, The M.S. University of Baroda, Vadodara, Gujarat, INDIA. 20 μL of each

sample was injected. The autosampler system (ekspertTM ultraLC 100 XL, eksigent-AB Sciex, USA) was tempered to 8°C equipped with column oven (ekspertTM ultraLC 100, eksigent-AB Sciex, USA) fixed at 40°C. Chromatographic elution of analyte was achieved using a Phenomenax C18 5µm (250*4.6) mm column at a flow rate of 0.5 ml/min for having run time 8 mins. The isocratic composition of eluent a (water with 0.1% formic acid) and eluent b (methanol) was in 60:40 % v/v.

4.1.2.2.2. LC-MS Conditions

Analysis was conducted using 3200 QTRAP mass spectrometer (AB Sciex, USA) equipped with electro spray ionization (ESI) source. The mass spectrometer was operated in the positive ion mode with a potential of 5.5 kV applied on the electro spray ionization needle. The ionization source temperature was 600 °C. ACV was identified and quantified using Multiple Reaction Monitoring (MRM) mode. The curtain gas (CUR) was at 25.0 psi, the nebulizer source gas 1 at 50.0 psi and the turbo ion source gas 2 at 50.0 psi was utilized. The optimized Declustering potential and entrance potential were 60.0 V and 5.6 V respectively. ACV fragmentation was achieved by collisionally activated dissociation (CAD) with nitrogen gas. The collision gas pressure was fixed at 2.0 psi for MRM quantitation. The collision energy 22.0 V and collision cell exit potential 3.0 V were optimized. Dwell time 200 ms was used. The product ion at m/z 226.00 was selected.

4.1.2.2.3. Preparation of Stock Solutions, Calibration and Validation Standards

An accurately weighed amount of ACV was transferred into a 10 mL calibrated flask and dissolved in 5 mL of mobile phase. The resulting solution were completed to the mark with mobile phase obtaining stock standard solution containing 1000 µg/mL. Stock solution

were then further diluted with mobile phase to obtain the working standard solutions at concentrations over the range of 50–1600 ng/mL. Six calibration standards were prepared at concentrations of 50, 100, 200, 400, 800 and 1600 ng/mL. Validation standards were similarly prepared at levels of 100, 200, 400 and 800 ng/mL.

4.1.2.2.4. Caco-2 cell line sample preparation

The samples for the ACV permeation studies were collected at different time points from the basolateral side from the transwell plates. The collected samples were filtered and diluted with the mobile phase. The prepared samples with unknown concentrations has been injected. The formulation samples were prepared by crushing twenty tablets up to fine powder and then an accurately weighed quantity of the powdered tablet contents equivalent to 10 mg of the active ingredient was transferred into a 10 mL calibrated flask and dissolved in about 6 mL of mobile phase. The contents of the flask were swirled, sonicated up to 9 minutes and then volume of the flask was made up with mobile phase. The mixture was mixed well, filtered and first portion of the filtrate was rejected. The prepared solution was diluted quantitatively with the mobile phase to obtain a suitable concentration for analysis.

4.1.2.2.5. Plasma sample preparation

Plasma extraction

ACV was extracted from plasma by protein precipitation, as shown in Figure 4.2. The protein in plasma sample (200 µl) was precipitated by adding acetonitrile (800 µl) and vortex mixed for 5 mins followed by centrifugation (10,000 rpm 10 min, 4 °C) and supernatant was collected. The supernatant was dried by exposure of nitrogen and then reconstituted in mobile phase. Final solution was injected into the LC-MS/MS.

Extraction efficiency

The extraction efficiency was calculated by adding known amount of ACV in plasma. The known amount of samples were injected in LC-MS and then the peak area of the samples with plasma and without plasma were compared.

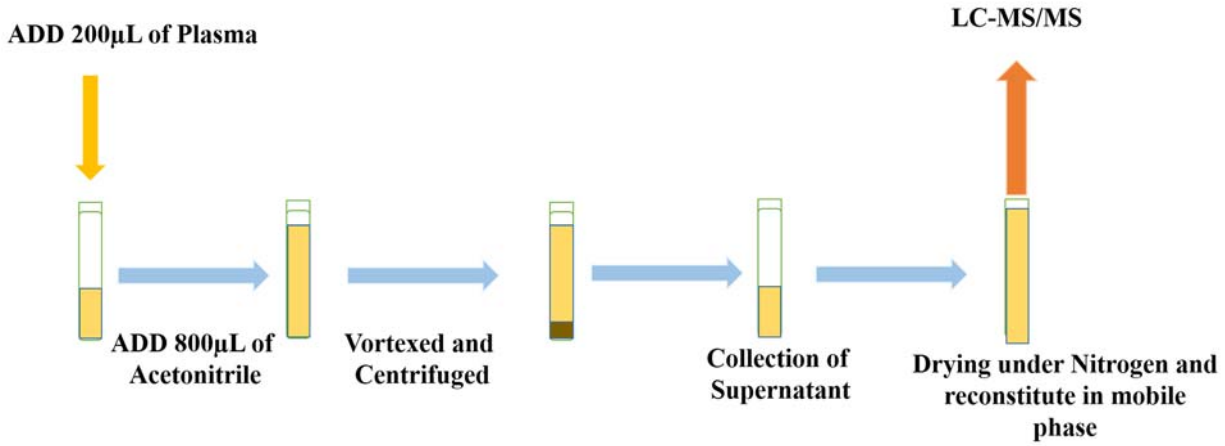

Figure 4.2 Plasma Extraction Procedure for ACV

4.1.2.2.6. Validation Procedures using total error approach

The present method was validated as per ICH guidelines and ISO guidelines which were grounded upon "total error" approach. In this approach "total error" was estimated by merging the systemic error and random error to recognize the difference between observed and true value. In the proposed method sensitivity of the method and effect of sample matrix were also studied. The selectivity of the developed method for cell line samples was investigated by comparing chromatograms of blank cell lines without ACV, blank mobile phase and sample of cell lines with ACV and sample of formulation as shown in Figure 4.3. While for plasma samples blank plasma, standard and sample were compared as shown in Figure 4.4. Response function in proposed method four sets of calibration curve were plotted between area and different concentrations of ACV and on these four different series regression analysis was performed and series with best coefficient of

determination was selected and the selected series has been further diagnosed by Lack of Fit (LOF) test and standard residual plot. Trueness of calibration curve was calculated by back calculation of concentrations to justify the calibration line. The results of trueness were expressed in terms of absolute and relative bias. The recovery study which is the most critical parameter in method validation requires an extra precautions during study and interpretation of recovery results. Therefore, the results of accuracy studies were interpreted and represented in the β-expectation tolerance limits. In addition to these parameters, risk profile has also been studied to know the future application of the method. Limit of detection and quantification represents the sensitivity of the method which has been calculated as per ICH guidelines. Subsequently confirmation of method fitness for the estimation of ACV in different matrix was carried out by analyzing market formulation and cell line samples.

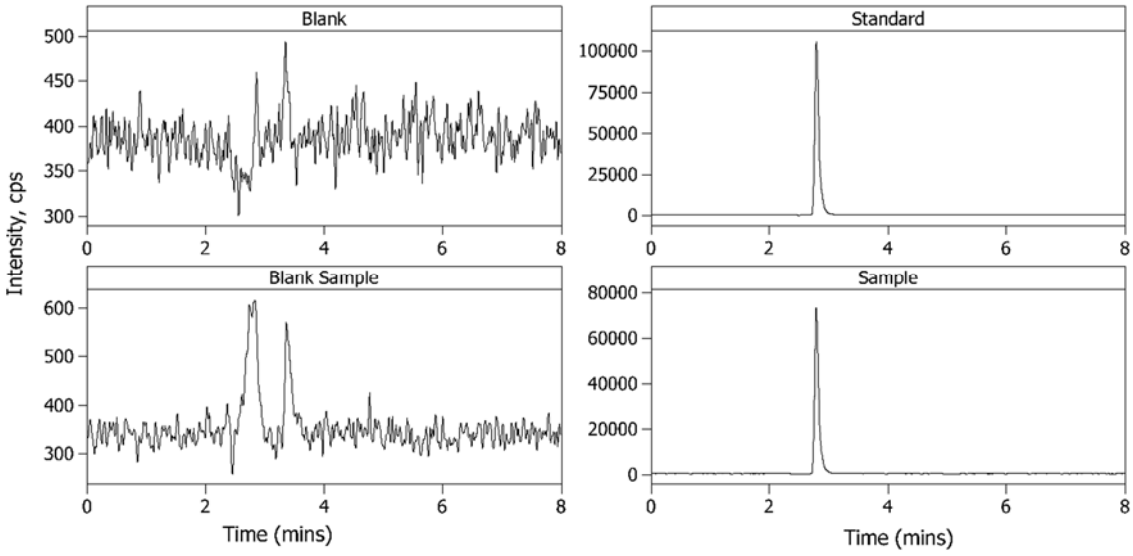

Figure 4.3 Chromatogram of blank, blank sample cell line, standard and sample.

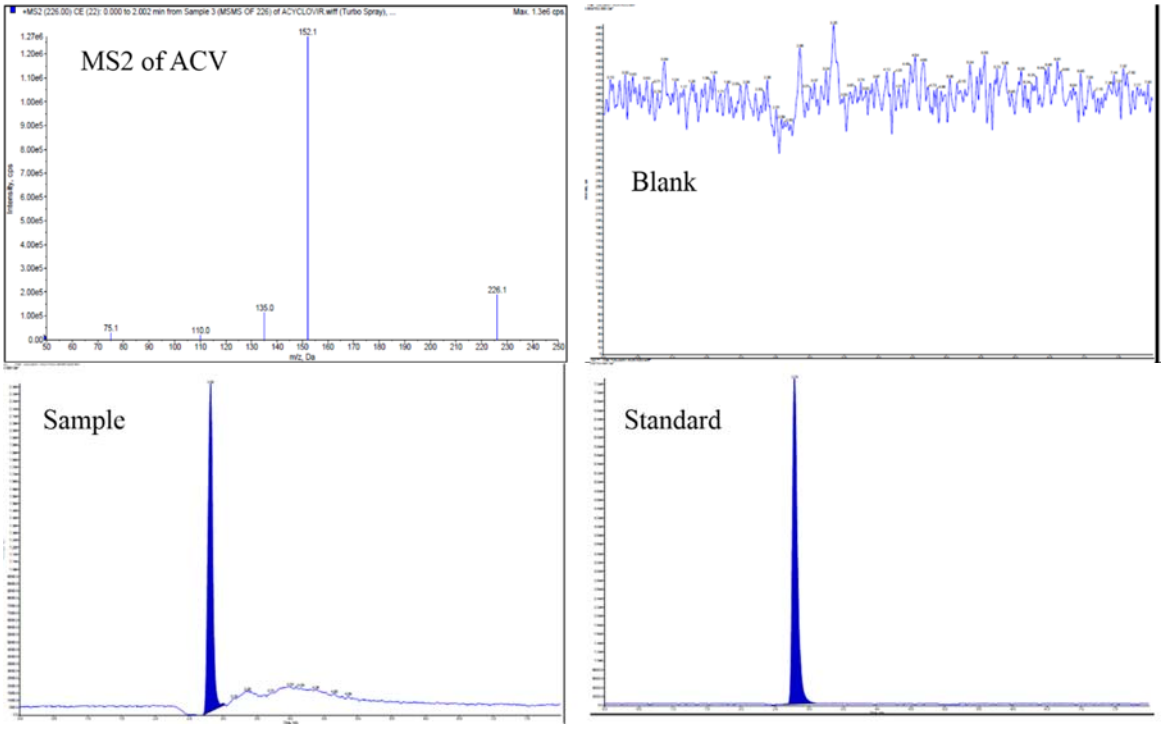

Figure 4.4 Chromatogram of blank, standard and plasma sample with MS2 of ACV

4.1.2.2.7. Uncertainty Estimation

4.1.2.2.7.1. Cause-effect diagram

Even though estimation method was validated as per guidelines but still doubt was there in results as during the validation of method small influences which can affect the results has not been studied, such as error during sample weighing, discharge of volumetric flask etc. Therefore, to overwhelm such doubts during result collation were clarified by estimation of uncertainty in results obtained from validation. The protocol for uncertainty estimation starts with identification of sources of uncertainty. The best way of listing uncertainty sources is to use the cause-effect diagram plan, as it outlines the sources connection to each other demonstrating their impact on the result. Thus a cause-effect diagram was assembled as presented in Figure 4.5. The parameters taken in consideration were volume of volumetric flask V_{10}, concentration of analyte C_{10}, and mass of sample,

recovery of method R_m and precision of method. This diagram also help in resolving any repeatability of components in uncertainty. The parameters comes in consideration after constructing cause-effect diagram were illustrated in Eq. 4.1. These identified sources were quantified and their discrete effect of on inclusive uncertainty was calculated and assembled as CSU and EU.

4.1.2.2.8. Individual parameters showing effect on overall uncertainty

4.1.2.2.8.1. Liberation of ACV solution from volumetric flask

The uncertainty due to liberation of volumetric flask was evaluated by performing experiment involving filling up and weighing of 10 mL volumetric flask with standard ACV solution for 10 times.

4.1.2.2.8.2. ACV mass (m_{sample})

Difference between weighing glass with and without the ACV sample provide the ACV sample mass.

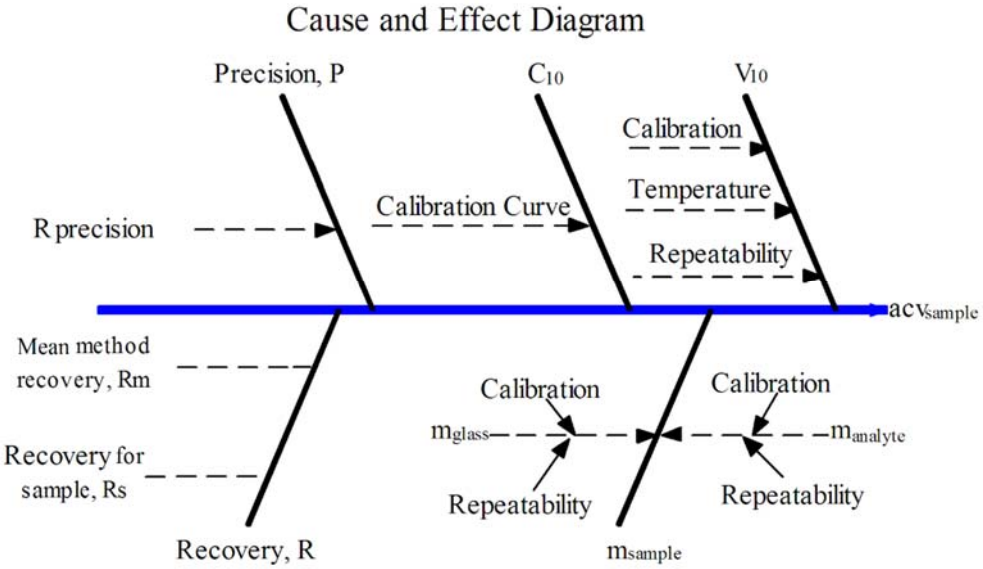

Figure 4.5 Cause and effect diagram to identify the sources of uncertainty

4.1.2.2.8.3. Concentration of ACV, C_{10}

The uncertainty in concentration of ACV obtained from calibration curve is expressed as uncertainty due to concentration C_{10}. This is estimated using Eq. 4.4 described in section 4.1.2.1.9.3.

4.1.2.2.8.4. Recovery of method

Uncertainty associated with recovery of method was evaluated using Eq. 4.3 as described in section 4.1.2.1.9.2 and it depends upon spiked and recovered concentration of standard in sample matrix.

4.1.3. Preparation of Physical Mixture of acyclovir and bioenhancers

The binary systems of ACV and bioenhancers were prepared in different weight ratios. ACV–QU, ACV–Sil, ACV–LT binary system were prepared at the five different weight ratio levels 5:0.5, 5:1, 5:1.5, 5:2, 5:2.5, 5:3 w/w. Physical mixture method was adapted for the binary system, in this the required amounts were accurately weighed and were sealed in a polythene bag and were blended for 30 minutes. All the prepared mixture were tested for uniformity of content using UV-Spectroscopy method for the ACV.

4.1.3.1 Compatibility studies of binary system

ACV–QU, ACV–Sil, ACV–LT binary system were studied for the compatibility of ACV with different bioenhancers. To carry out these studies Fourier Transform Infrared Spectroscopy (FTIR) and Differential Scanning Calorimetry **(**DSC) instrumentation were used. The FTIR spectrum of the ACV and binary mixtures were recorded and were interpreted for any physical interaction. Similarly the DSC chromatogram for the ACV and binary mixtures were recorded and were interpreted for physical interaction.

4.1.3.1.1. Fourier Transform Infrared Spectroscopy (FTIR)

FTIR transmission spectra of a pure ACV, QU, Sil, LT, ACV–QU, ACV–Sil and ACV–LT and binary systems of PM method were obtained using Avatar™ 360 E.S.P™ FTIR spectrometer, Thermo Nicolet Corp., Madison, WI, USA. Samples were mixed with dry KBr in 1:100 and converted to a fine powder before compressing into KBr disc. Each sample was scanned for 16 times over a wave number region of 500–4000 cm^{-1}. The characteristic peaks of ACV were observed and compared with the spectrum of binary mixtures to check any physical interaction among the ACV and bioenhancers.

4.1.3.1.2. Differential Scanning Calorimetry (DSC)

The DSC thermograms of ACV, Sil, QU, LT and their binary systems were recorded and saved in the range of 0-350ºC using Mettler-Toledo, Schwerzenbach, Switzerland. During the recording of thermograms an empty aluminium pan was used as the reference for the samples. The rate of heating was kept 10 °C min^{-1}.

4.1.4. *Ex-vivo* permeation studies

In the *Ex-vivo* permeation studies Franz diffusion cell with an area of 3.80 cm^2 having donor and acceptor compartment were used as shown in Figure 4.6. The intestinal tissue of goat was collected from local slaughter house and was stored in normal saline. Tissue was cleaned and intestinal content was removed by a slow infusion of normal saline and air before setting up for the experimentation. The prepared binary systems using the physical mixture method was assessed for the permeation using the intestinal tissue of the goat which is very much morphological similar to human intestine tissue. In this experimentation the tissue was mounted in between the donor and acceptor chamber in the diffusion cell. The donor compartment was filled with the sample (ACV and binary

systems) having concentration (10 mg/ml) and acceptor cell was filled up with the simulated intestinal fluid (SIF) with aid to continuous stirring of 600 rpm and then samples from the acceptor compartment (1 mL each) were withdrawn at different time intervals (0, 15, 30, 60, 120, 180, 240, 360, 480 min) and filtered using the syringe filters. The ACV amount was quantified using validated LC-MS method for the ACV as described earlier in this chapter. The amount of the drug permeated through the tissue was determined. The amount permeated was plotted against the different time points. The permeability coefficients (Peff) and permeation enhancement ratios (ER) (from Peff values) were calculated as per Eq. 4.6 and 4.7 respectively for all the experiments (n=3).

$$Peff\,(cm/\sec) = \frac{dQ/dt}{A*Cd} \tag{4.6}$$

Where, A = the surface area, dQ/dt = amount of drug permeated per unit time at steady state, Cd = donor drug concentration.

$$R = \frac{Papp(sample)}{Papp(control)} \tag{4.7}$$

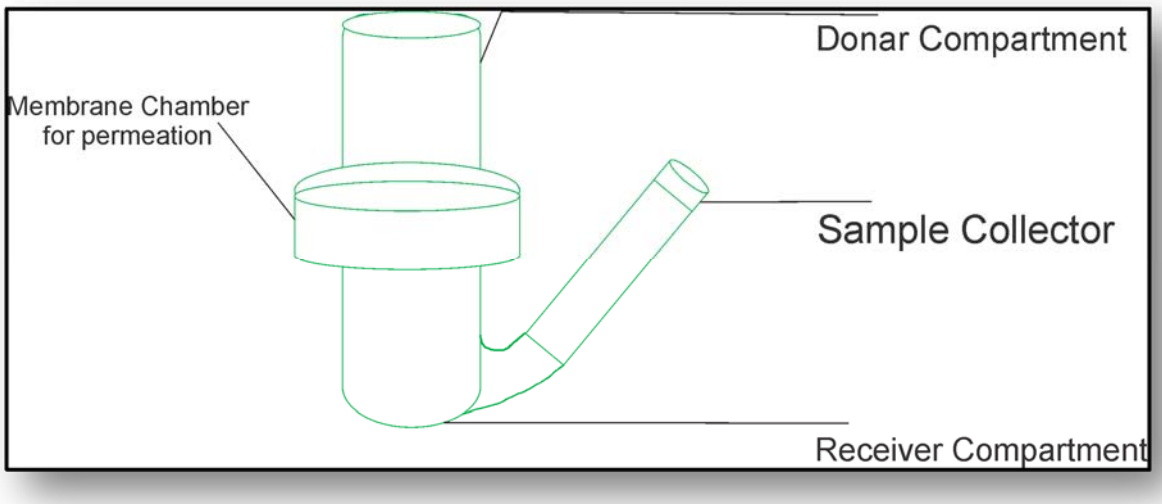

Figure 4.6 Diffusion cell design for *ex-vivo* permeation studies

4.1.5. Cellular Uptake and Transport of ACV across the Caco-2 cell monolayers

In Caco-2 cell lines studies, a monolayer of cells is grown on the filter which is separating two parts (donor and acceptor) of a micro sized well in the plates as shown in Figure 4.7. Generally plates used for these studies are called as Trans well plates. These cell lines are used to study the permeation of the drug compounds from one side of the plate to the other after the addition of sample. The Caco-2 cell line preferred as because it has a very welly separated border on apical surface and tight junctions.

This cell line model is simple and very highly reproducible. This cell line model has been recognized by US FDA for the study of permeation of drug compounds in the process of bioequivalence waiver.

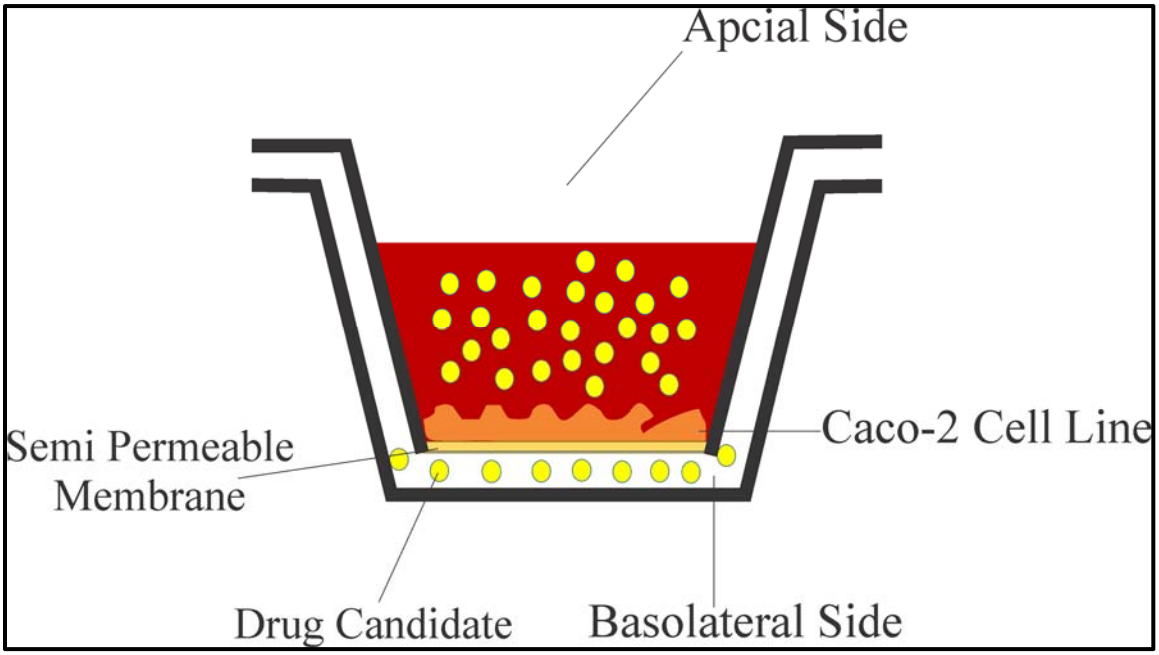

Figure 4.7 Transwell Plate containing Caco-2 cell lines

Caco-2 cell line exhibits several advantages over conventional ways to predict permeation. It provides a rapid access to the drug candidate's permeability. It also helps in prediction

of pathways for drug transportation. It also helps to find out the toxic effects of drug candidates on the same biological barrier.

4.1.5.1. Material

Caco-2 cell line studies were conducted at Stem Cure laboratory, Ahmedabad. Caco-2 cell line was procured from NCCS Pune. Cell culture reagents included trypsin solution, Hanks balanced salt solution, and phosphate buffered saline (PBS) were prepared at Stem cure laboratory. Cell media Dulbecco's modified Eagle medium (DMEM), non-essential amino acids (NEAA), fetal bovine serum (FBS), L-glutamine, penicillin, streptomycin solution were purchased from Sigma Aldrich Ltd. (Ayrshire, UK). Cell culture flasks were obtained from Stem cure laboratory. Transwell cell culture plates with filter inserts (12 wells, 1.12 cm^2 polyester having 0.4 μm pore size) were purchased from Costar, Corning Inc. (Sigma aldrich).

4.1.5.2. Cell Culture Protocol

Caco-2 cells were cultured and prepared for permeation studies as per published method (12). Caco-2 cell lines were cultured in Dulbecco's modified Eagle's medium (DMEM) supplemented with high glucose, fetal bovine serum, penicillin, and streptomycin at 37 °C and 5% CO_2. The Caco-2 cells were seeded at the density of approximately 1×10^5 cells per well in to a 12-well transwell polycarbonate cell culture inserts having 12-mm diameter and 4-μm pore size purchased from Costar®, (Corning Costar Co, Cambridge, MA, USA). The cells were cultured and used after 25 days so that full maturation and confluence must obtained. It also includes P-glycoprotein (P-gp) expression and the formation of tight junctions in the cell monolayer. For the very first week of the culturing the medium was

replaced every other day. After 7 days the medium was changed daily. The basolateral (BL) and apical (AP) compartments contained 1.5 and 0.5 mL of culture medium, respectively.

Cellular uptake

In trailing the cellular uptake of ACV and binary systems the fluorescein labeled samples were prepared using rhodamine B using anti-solvent precipitation method. In this study, cells were treated with test solutions up to 1 hr at 37ºC. After 0, 0.5 and 1 hr samples were removed from the well and cell line was washed using HBBS. Cells were then treated with paraformaldehyde solution for 10 min and then stain with 5 µg/ml solution of 4,6-diamidino-2-phenylindole (DAPI) and then images were recorded under the confocal laser scanning microscope (CLSM) (Olympus Japan) (13, 14).

Transport study

The trans-epithelial electric resistance (TEER) values were measured using Millicell®-ERS (Millipore, Bedford, MA, USA) before and immediately after the transport studies to evaluate the integrity of the Caco-2 cell monolayers. The transport medium (HBSS) resistance was subtracted from the TEER value considering it as the background resistance. The cell monolayers having TEER values below 300 $\Omega \cdot cm^2$ were excluded from the study design. The study design for ACV and binary system has been shown in Table 4.1, 4.2, 4.3 4.4, 4.5.

The cell monolayer was equilibrated at 37 °C with warm HBSS (37 °C) for 30 min before starting the experimentation (transport studies). After 30 mins, the HBSS was removed and the sample solutions (ACV, ACV-QU, ACV-Sil, and ACV-LT containing 10 µM/mL ACV in HBSS) were added to the AP compartments. Sample (100 µL) were withdrawn from the

receiver chamber at different time points (30, 60, 90, 120, 240, 480 mins) the equal volume (100 μL) of fresh HBSS was added to the chamber so as to maintain a constant volume. The drug concentration in the samples was determined by validated LC-MS method as described above. The experiments were performed in triplicate. The apparent permeability coefficient (Papp, cm/s) was calculated using the following Eq. 4.8.

$$Papp(cm/\sec) = \frac{dQ/dt}{A * C0} \qquad (4.8)$$

Where, dQ/dt is the transport rate, C0 is the initial drug concentration on the apical side, and A is the surface area of the membrane filter (1.12 cm^2).

Cell Viability estimation

At the end of the experimentation, cell viability for the cell lines were checked using tryphan blue (15) staining technique. The viability of cells treated with ACV and binary systems were greater than 90% and not significantly different from the control cells. Trypan blue chromophore is negatively charged so it does not react with the membrane until it is damaged, so all the cells that exclude the dye are viable.

Table 4.1 Study Design for Caco-2 cell lines (Plate No. 1)

A1 **HBSS (Blank)**	**B1** 10 μM ACV	**C1** ACV:QU (5: 0.5)	**D1** ACV:QU (5: 1)
A2 **HBSS (Blank)**	**B2** 10 μM ACV	**C2** ACV:QU (5: 0.5)	**D2** ACV:QU (5: 1)
A3 **HBSS (Blank)**	**B3** 10 μM ACV	**C3** ACV:QU (5: 0.5)	**D3** ACV:QU (5: 1)

Table 4.2 Study Design for Caco-2 cell lines (Plate No. 2)

A1 ACV:QU (5: 1.5)	**B1** ACV:QU (5:2)	**C1** ACV:QU (5: 2.5)	**D1** ACV:QU (5: 3)
A2 ACV:QU (5: 1.5)	**B2** ACV:QU (5:2)	**C2** ACV:QU (5: 2.5)	**D2** ACV:QU (5: 3)
A3 ACV:QU (5: 1.5)	**B3** ACV:QU (5:2)	**C3** ACV:QU (5: 2.5)	**D3** ACV:QU (5: 3)

Table 4.3 Study Design for Caco-2 cell lines (Plate No. 3)

A1 ACV:Sil (5: 0.5)	**B1** ACV:Sil (5:1)	**C1** ACV:Sil (5: 1.5)	**D1** ACV:Sil (5: 2)
A2 ACV:Sil (5: 0.5)	**B2** ACV:Sil (5:1)	**C2** ACV:Sil (5: 1.5)	**D2** ACV:Sil (5: 2)
A3 ACV:Sil (5: 0.5)	**B3** ACV:Sil (5:1)	**C3** ACV:Sil (5: 1.5)	**D3** ACV:Sil (5: 2)

Table 4.4 Study Design for Caco-2 cell lines (Plate No. 4)

A1 ACV:Sil (5: 2.5)	**B1** ACV:Sil (5:3)	**C1** ACV:LT (5: 0.5)	**D1** ACV:LT (5: 1)
A2 ACV:Sil (5: 2.5)	**B2** ACV:Sil (5:3)	**C2** ACV:LT (5: 0.5)	**D2** ACV:LT (5: 1)
A3 ACV:Sil (5: 2.5)	**B3** ACV:Sil (5:3)	**C3** ACV:LT (5: 0.5)	**D3** ACV:LT (5: 1)

Table 4.5 Study Design for Caco-2 cell lines (Plate No. 5)

A1 ACV:LT (5: 1.5)	**B1** ACV:LT (5:2)	**C1** ACV:LT (5: 2.5)	**D1** ACV:LT (5: 3)
A2 ACV:LT (5: 1.5)	**B2** ACV:LT (5:2)	**C2** ACV:LT (5: 2.5)	**D2** ACV:LT (5: 3)
A3 ACV:LT (5: 1.5)	**B3** ACV:LT (5:2)	**C3** ACV:LT (5: 2.5)	**D3** ACV:LT (5: 3)

4.1.6. *In vivo* pharmacokinetic study in rabbits

4.1.6.1. Animal preparation for *In-vivo* studies

In vivo pharmacokinetic study performed in New Zealand white rabbits (2-3 Kg) provided by the animal house at Pharmacy Department, The Maharaja Sayajirao university of Baroda details has been provided in Table 4.6. All the experiments were performed under guidelines approved by the Institutional Animal Ethics Committee (IAEC Registration number 404/01/a/CPCSEA). The rabbits were given free access to food and water. The rabbits were fasted for 12 h prior to the experiments with free access to water.

Table 4.6 Animals detail used for pharmacokinetic Studies

Species/Common name	New Zealand White Rabbits
Age/Weight/Size	3-4 months/2 – 3 Kg
Gender	Either sex
Number of animals to be used	15
Proposed source of animals	CPCSEA approved breeding facility

4.1.6.2. Dosing

In pharmacokinetics study rabbits were divided in to five groups (3 per group). Grouping has been shown in Table 4.7. The ACV (oral), ACV (IV), ACV:QU, ACV:Sil, ACV:LT were orally administered as suspension, at a dose of 40 mg/kg. The rabbits had free access to water during the entire experiment. Blood samples of 600 µL were collected at 0.5, 1, 1.5, 2, 3, 4, 6, 8, 10, 12 and 24 hr after dosing via the orbital venous plexus using isoflurane as anesthesia. The whole blood was collected in heparinized tubes, and the plasma from the sample was separated by centrifugation at 10000 rpm for 10 min and stored at -20 °C prior to analysis by LC-MS.

Table 4.7 Dosing details for pharmacokinetic studies

S.no	Groups	Dose	Route	Total number of animals
1	Control	ACV (40mg/kg)	Oral	3 Rabbits
2	ACV:QU	5:2	Oral	3 Rabbits
3	ACV:Sil	5:1	Oral	3 Rabbits
4	ACV:LT	2:2.5	Oral	3 Rabbits
5	I.V	Acyclovir (3mg/kg)	I.V	3 Rabbits

4.1.6.3. Analysis of plasma samples

The concentration of ACV in the plasma samples were estimated by LC-MS. The extraction for the analysis of sample was carried out using protein precipitation method as described above. The drug concentrations in the samples were calculated as described above.

4.1.6.4. Pharmacokinetic and Statistical analysis

The drug concentration obtained from the LC-MS analysis was used to derive pharmacokinetic parameters. WinNonlin 6.3 was used to determined parameters maximum plasma concentration (Cmax), time for maximum plasma concentration (Tmax), Area under the curve (AUC) etc. All other mathematical calculations were done using the Microsoft Excel 2013.

4.1.6.4.1. Pharmacokinetic parameters estimated

4.6.4.1.1. Maximum plasma concentration (Cmax)

Maximum plasma concentration was determined directly using the plasma concentration time profiles. The maximum plasma concentration was known as maximum concentration of ACV obtained in plasma samples estimated using LC-MS.

4.6.4.1.2. Time to maximum plasma concentration (Tmax)

Time to maximum plasma concentration was determined directly using the plasma concentration time profiles. *Tmax* was known as the time point at which the maximum concentration of ACV was obtained from plasma concentration profile. It can also be calculated by time corresponds to Cmax.

4.6.4.1.3. Area under the plasma concentration-time curve

Area under curve was calculated using trapezoidal rule. According to this area under the curve from time t_2 to time t_1 is calculated using Eq. 4.9.

$$AUC_{t1}^{t2} = \left(\frac{C_1 + C_2}{2} \right) \times (t_1 - t_2) \qquad (4.9)$$

Where, C_1 and C_2 are concentrations at time t_1 and t_2.

4.6.4.1.4. Relative Bioavailability (%)

The *in vivo* performance of ACV was compared with the binary systems in the terms of relative bioavailability. The relative bioavailability was calculated using Eq. 4.10.

$$\text{Re}\,lativeBA\,(\%) = \frac{AUC\,(binarysyst\ em)}{AUC\,(ACV)}\,X\,\frac{Dose\,(reference)}{Dose\,(test)} \quad (4.10)$$

4.2. Results and discussion

4.2.2. Analytical and Bio-analytical Method development and Validation

4.2.2.1. Zero order UV Spectroscopy method

The absorption spectrum of ACV was recorded and it shows maximum absorption intensity at 257nm. Thus all the studies were carried out at the same wavelength (nm).

4.2.2.1.1. Validation parameters

4.2.2.1.1.1. Response function (calibration curve)

In the proposed method calibration curves were prepared using linear regression model. Four different sets were prepared for response function studies within range of ACV from 2--12 µg/mL. As four sets were prepared, all of them were found to be following the linear regression model and their regression analysis parameters results were studied. As from regression analysis studies, series 4 shows the best coefficient of determination r^2 as 0.9999 with regression equation (Y = 0.08083X – 0.001444), was selected for further studies and computation. Furthermore, the linear regression model is also confirmed for its suitability for method by diagnosis using Lack of Fit (LOF) test and Levene's test. As *p*-values were found to be higher than 0.05, represented in Table 4.8 to demonstrate that no outliers were found in calibration curve, standard residual plot was also plotted as shown in Figure 4.8. Now to confirm the chosen regression equation, back calculation was done and linear plot based upon absolute β-expectation limit was generated between nominal and back calculated concentration which shows r^2 value is 0.9998 and it becomes clear that the calibration lines adequately describe the observed relationship.

4.2.2.1.1.2. Trueness

To justify the trueness of the method percentage relative bias was calculated and is illustrated in Table 4.9 from where it can be concluded that the trueness for all different concentration is acceptable, since the percentage relative bias is limited between -0.641% and 1.87%.

Table 4.8 Results of LOF and Levene's test for linear regression model

Test	Error	SS	df	MS	Fcalc	Fcrit,95%	p-value
Lack of Fit	LOF Error	0.0001047	16	0.00000873	1.775	1.918	0.1046
	Pure Error	0.0001475	38	0.00000492			
Levene's	Model	0.0000142	5	0.00000285	1.886	2.380	0.1173
	Error	0.0000634	56	0.00000151			

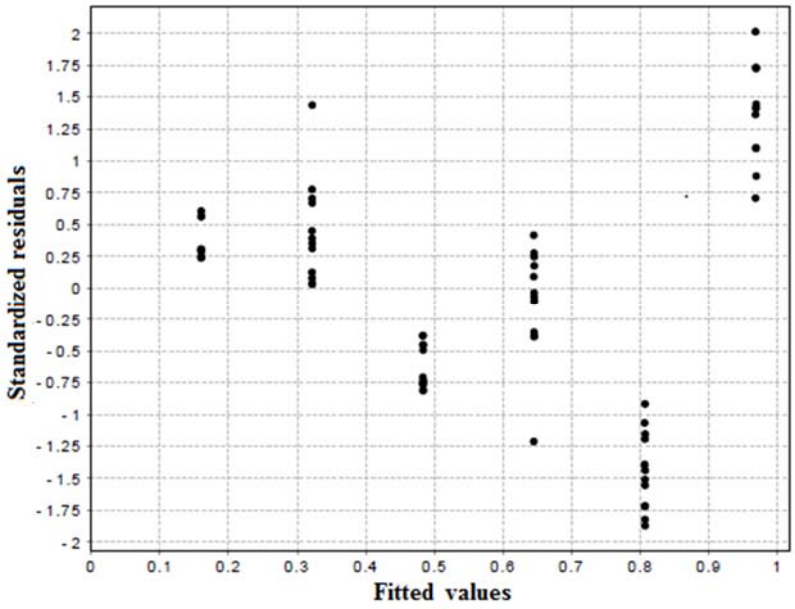

Figure 4.8 Standard residual plot of four different series representing absence of outliers in all different concentration levels

Table 4.9 Results of Trueness in terms of relative bias (%)

Nominal concentration (µg/mL)	**Back calculated concentration (µg/mL)**	**Absolute bias (µg/mL)**	**Relative bias (%)**
2.000	2.038	0.03754	1.877
4.000	3.952	-0.04821	-1.205
6.000	5.974	-0.02588	-0.4313
8.000	7.949	-0.05130	-0.6413
10.00	10.04	0.03764	0.3764
12.00	12.00	0.000905	0.00754

4.2.2.1.1.3. Accuracy

The accuracy of the method was carried out by standard addition method. Accuracy takes into account the total error of the test results and is represented by the β-expectation tolerance limits. The method accuracy was performed using different matrices and thus accuracy obtained by considering linear regression model has been summarized in Table 4.10. It was also found that the β-expectation tolerance limits do not exceed the acceptance limits which means that β-percent (95%) of the future measurement of unknown samples will be included within the tolerance limits as shown by accuracy profile illustrated in Figure 4.9. Accuracy profile of the method was also justified by risk profile by choosing maximum risk level at 5.0% and it was concluded that the risk of outliers are within limits and future analysis of unknown sample will fall within the range. To evaluate the errors in intra accuracy studies a linear plot was also generated which shows the linearity between

nominal and observed concentrations with r^2 as 0.9989 and also confirm the outliers in different spiking concentrations a standard residual plot was drawn which shows that there are no outliers falling in the intra accuracy studies as shown in Figure. 4.10.

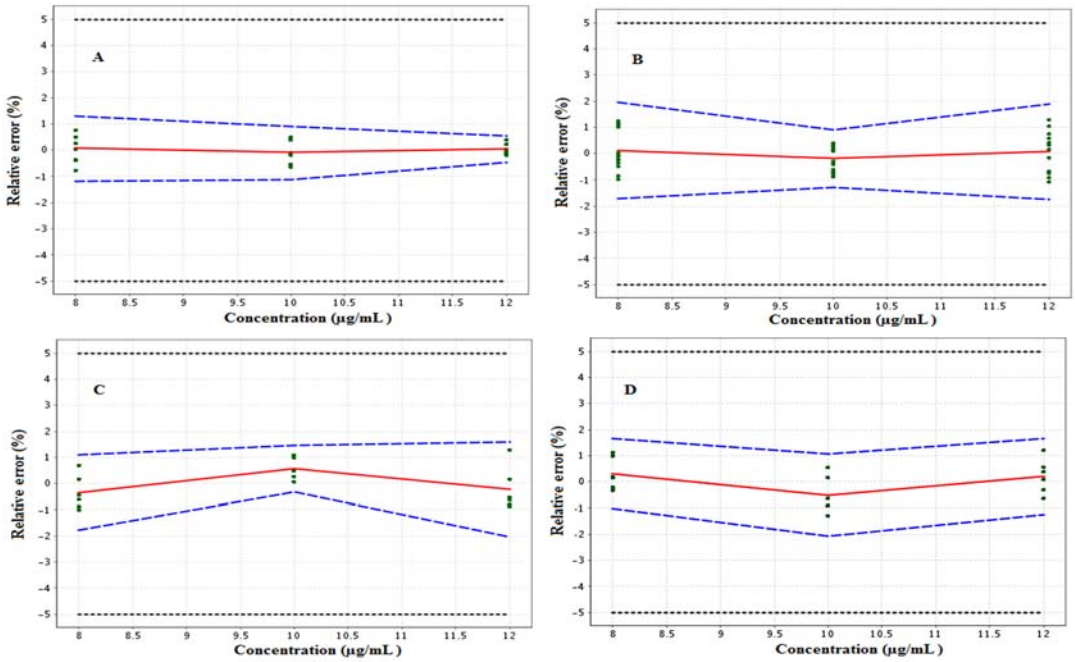

Figure 4.9 Accuracy profile of acyclovir determination in A) tablets B) skin cream C) eye ointment D) injection obtained after application of linear regression using calibration standards prepared with the matrix. The plain line is the relative bias, the dashed lines are the 95% β-expectation tolerance limits and the dotted curves represent the acceptance limits (± 5%). The dots represent the relative back calculated concentrations of the validation standards.

Table 4.10 Result of method accuracy in terms of relative beta-expectation tolerance limit and risk assessment obtained by selected regression model in different matrix

Matrix	Concentration Level (%)	Concentration (µg/mL)	Beta-expectation tolerance limits (µg/mL)	Relative Beta-expectation tolerance limits (%)	Risk[a] (%)
Tablet	80.0	8.000	[7.91 , 8.10]	[-1.17 , 1.30]	0.000339
	100.0	10.00	[9.89 , 10.09]	[-1.10 , 0.90]	0.000048
	120.0	12.00	[11.95 , 12.06]	[-0.44 , 0.52]	0.00000003
Cream	80.0	8.000	[7.92 , 8.13]	[-1.02 , 1.65]	0.000832
	100.0	10.00	[9.79 , 10.10]	[-2.06 , 1.05]	0.003895
	120.0	12.00	[11.85 , 12.20]	[-1.24 , 1.66]	0.001583
Ointment	80.0	8.000	[7.86 , 8.09]	[-1.78 , 1.08]	0.001602
	100.0	10.00	[9.97 , 10.15]	[-0.34 , 1.45]	0.000029
	120.0	12.00	[11.75 , 12.19]	[-2.05 , 1.59]	0.01124
Injection	80.0	8.000	[7.92 , 8.13]	[-0.98 , 1.62]	0.00066
	100.0	10.00	[9.80 , 10.09]	[-1.97 , 0.94]	0.002294
	120.0	12.00	[11.85 , 12.21]	[-1.28 , 1.71]	0.002071

[a]Risk of having measurements falling outside of the acceptance limits (± 5%)

4.2.2.1.1.4. Limit of detection and quantification

Results of LOD and LOQ show that this method is sensitive enough to analyze the marketed formulations. Values of LOD and LOQ were found to be 0.255 and 0.772 µg/mL respectively.

4.2.2.1.1.5. Robustness studies

Robustness of the developed method was determined in the form of percentage RSD by small but deliberate changes in the solvent grade and detection wavelength in all the sample matrices. The results of robustness studies are represented in Table 4.11 showing the effect of variation on amount found in sample matrix and from these results it was concluded that the method has enough capacity to bear up to an extent human or system errors.

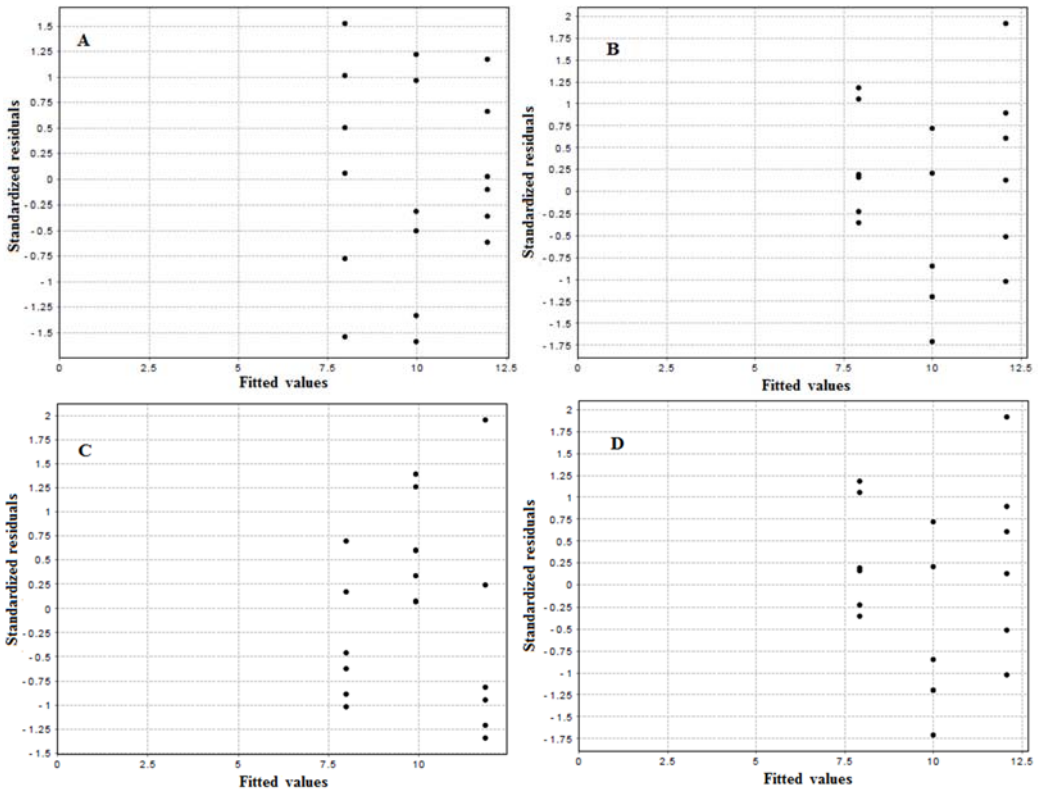

Figure 4.10 Standard residual plot confirming absence of outliers in determination of accuracy of A) tablets B) skin cream C) eye ointment D) injection.

Table 4.11 Result of robustness studies in different variations in terms of mean concentration found and %RSD (n=6)

Parameters Studied		Nominal Conc (ug/mL)	Mean Conc Found (ug/mL) ± %RSD			
			Tab.	Crm.	Ont.	inj
	HPLC	10	9.98 ± 0.79	10.01 ± 0.32	9.99 ± 0.35	9.98 ± 0.35
Solvent	SD*	10	9.96 ± 0.44	9.94 ± 0.56	9.98 ± 0.71	10.01 ± 0.65
Grade	DD*	10	9.93 ± 0.64	9.93 ± 0.33	10.02 ± 0.51	9.99 ± 0.53
	256	10	9.96 ± 0.60	9.91 ± 0.41	9.97 ± 0.80	9.93 ± 0.59
ƛ max	257	10	9.95 ± 0.91	9.91 ± 0.91	9.98 ± 0.42	9.99 ± 0.63
(nm)	258	10	9.95 ± 0.90	9.96 ± 0.90	9.97 ± 0.86	9.96 ± 0.42

Tab-Tablet, Crm- Skin Cream, Ont- Eye Ointment, inj-injection *SD-Single distilled, *DD-Double distilled

4.2.2.1.1.6. Precision

The results of precision were found to be < 2% in terms of RSD for both repeatability and intermediate levels. These results of intermediate and repeatability precision suggest that developed analytical method was precise and reproducible. Results has been shown in Table 4.12.

4.2.2.1.2. Application of the proposed method to analysis of dosage forms

4.2.2.1.2.1Sonication time optimization

As the matrices are different so the extraction time of ACV from them will be different. To achieve maximum extraction of ACV, optimization of sonication time was carried out by analyzing samples after different sonication times. The most suitable sonication time for tablet, skin cream, eye ointment and injection was found to be 9, 15, 20, 9 min, respectively. After sonication for these particular time period, percentage purity for all formulations was found to be in the range of 99 –101%.

4.2.2.1.2.2. Analysis of dosage form

It is evident from the aforementioned results that proposed method gave satisfactory results with the drug. The percentage purity for skin cream, eye ointment, tablet and injection were found to be 99.75, 101.36, 100.9 and 99.21, respectively. It is evident from the above mentioned values that proposed method is applicable to the analysis of drug in its bulk and dosage forms with comparable analytical performance.

4.2.2.1.3. Measurement of uncertainty

After the uncertainty sources were identified according to the cause-effect diagram, these were evaluated, their magnitude was determined and in order to assure the traceability for uncertainty results all the calculation were done in International System of Units as concentration in M and weight in kg.

4.2.2.1.3.1. Uncertainty due to concentration, c_{10}

After the scanning of standard solution, values in terms of absorbance were obtained and calibration curve was plotted as described by Eq. 4.4. Regression equation of calibration curve was identified as, slope 10746 and intercept 0.079. For the determination of calibration curve, six solutions were measured three times (total number of measurements, n=18). The sample solution was measured ten times, thus obtaining analyte concentration in tablet, cream, ointment and injection and results are represented in Table 4.13.

$$S_{xx} = 1.142 \times 10^{-9}$$

$$S_r = 3.037 \times 10^{-2}$$

Then using S_r and S_{xx}, standard relative uncertainty due to concentration was calculated and results are expressed in Table 4.14. A very small difference was observed in the standard relative uncertainty of different formulations.

4.2.2.1.3.2. Uncertainty of the liberation of 10 mL volume of 10 mL volumetric flask

The effect on volume of 10 mL volumetric flask is mainly influenced by the three parameters i.e. calibration of the volumetric flask (at the time of manufacturing), repeatability and temperature.

4.2.2.1.3.3. Calibration of volumetric flask

Deviation of value from nominal volume for 10 mL volumetric flask was ± 0.007 mL (at 27 °C) as given by manufacturer and by assuming that standard deviation is not claimed by manufacturer with confidence interval limit, standard value of uncertainty can be calculated with triangular distribution. Thus, uncertainty associated with liberation of 10 mL volume of 10 mL volumetric flask due to calibration u (V_{10cal}) is shown in Eq. 4.11.

$$u\,(V_{10\,cal}) = \frac{0.007}{\sqrt{6}} = 2.86 \times 10^{-3}\text{mL} \qquad (4.11)$$

4.2.2.1.3.4. Repeatability u(V_{10}rep).

After filling and weighing of 10 mL volumetric flask, standard uncertainty of volumetric flask was established at 0.0014 mL.

Table 4.12 Results of relative and absolute intermediate precision and repeatability in terms of (%RSD)

Nominal Conc. (µg/mL)	Relative intermediate precision and repeatability				Absolute intermediate precision and repeatability			
	Rep* (%RSD)	IP# (%RSD)	95% upper confidence limit		Rep* (SD) (µg/mL)	Between-series (SD) (µg/mL)	Ration of variance components (between/within)	IP# (SD)(µg/mL)
			Rep* (SD) (µg/mL)	IP# (SD) (µg/mL)				
2.000	0.4252	0.5263	0.0161	0.0663	0.1183	0.0677	0.0136	0.0405
4.000	0.4857	0.5657	0.0353	0.0353	0.0473	0.0184	0.1521	0.0507
6.000	0.4184	0.5586	0.0937	0.0513	0.0395	0.0226	0.3277	0.0455
8.000	0.2134	0.2877	0.0662	0.0770	0.0227	0.0039	0.0304	0.0230
10.00	0.2544	0.3493	0.0822	0.0566	0.0514	0.0193	0.1402	0.0549
12.00	0.2152	0.3619	0.0750	0.0697	0.0630	0.0239	0.1441	0.0674

4.2.2.1.3.5. Temperature

The manufacturer has calibrated volumetric flask at the time of manufacturing at a temperature of 27°C, while temperature in the laboratory varied within a range of $\Delta t = \pm$ 4°C. This difference was overcome by calculating uncertainty value with estimation of temperature range and volume dilatation coefficient. Volume expansion of liquid was taken into consideration, as it is quite higher than expansion of volumetric flask. The volume expansion coefficient, γ, of water is 2.1×10^{-4} /°C. Thus uncertainty for 10 mL volumetric flask ΔV_{10} was calculated by Eq. 4.12.

$$\Delta V_{10} = V_{10} \times \gamma \times \Delta t \qquad (4.12)$$

Where ΔV_{10}, uncertainty of the 10 mL volumetric flask; V_{10}, volume of the 10 mL volumetric flask; γ, volume dilatation coefficient; Δt, temperature variation in the laboratory.

Thus, we obtain that uncertainty for volumetric flask of 10 mL is 0.0084 mL, also assuming temperature variation is rectangular distribution, and standard uncertainty for 10 mL volumetric flask due to the temperature effect will be u (V_{10temp}) as shown in Eq. 4.13.

$$u\left(V_{10-temp}\right) = \frac{4\times 2.1\times10^{-4}\times10}{\sqrt{3}} = 0.0048\text{mL} \qquad (4.13)$$

Thus, standard uncertainty due to liberation of 10 mL volume of 10 mL volumetric flask was calculated according to Eq. 4.14 and was found to be 0.0058 mL. Standard relative uncertainty was calculated and shown in Eq. 4.15.

$$u(V_{10}) = \sqrt{(u(V_{10-cal}))^2 + (u(V_{10-rep}))^2 + (u(V_{10-temp}))^2} \qquad (4.14)$$

$$u(V_{10}) = 0.0058 \text{ mL}$$

The standard relative uncertainty will be:

$$\frac{u(V_{10})}{V_{10}} = 5.76 \times 10^{-4} \qquad (4.15)$$

Table 4.13 Results of concentration determination of acyclovir in tablet, skin cream, eye ointment and injection

	Acyclovir found (g)				Concentration (M × 10^{-5})			
Sample No	Tablet	Skin Cream	Eye Ointment	Injection	Tablet	Skin Cream	Eye Ointment	Injection
1	0.01007	0.00982	0.00973	0.00996	4.08	3.97	3.94	4.03
2	0.01010	0.00977	0.00998	0.00998	4.08	3.95	4.04	4.04
3	0.01012	0.00987	0.00977	0.00994	4.09	3.99	3.95	4.02
4	0.01000	0.01005	0.01010	0.00989	4.05	4.07	4.08	4.00
5	0.01003	0.00996	0.00973	0.00987	4.06	4.03	3.94	3.99
6	0.01005	0.01007	0.01014	0.01005	4.07	4.08	4.10	4.07
7	0.00994	0.01012	0.01000	0.00994	4.02	4.09	4.05	4.02
8	0.00998	0.01000	0.00996	0.00998	4.04	4.05	4.03	4.04
9	0.01007	0.00973	0.00998	0.01007	4.08	3.94	4.04	4.08
10	0.00996	0.01007	0.00973	0.00996	4.03	4.08	3.94	4.03
Mean	0.01003	0.00995	0.00991	0.00996	4.06	4.02	4.01	4.03

4.2.2.1.3.6. Uncertainty associated with the sample mass m_{sample}

Estimation of sample mass has three types of uncertainty sources such as sensitivity, linearity, and repeatability. Mass of the sample was expressed in kg for convenient traceability of results.

4.2.2.1.3.7. Sensitivity

The range of difference in weighed mass was very less and the same weighing balance was used each time. Thus, uncertainty due to sensitivity of balance can be neglected.

4.2.2.1.3.8. Linearity

As the manufacturer data indicated a linearity value is 0.0001g thus, to determine overall uncertainty value, standard uncertainty due to linearity was considered. A rectangular distribution was assumed to convert contribution of linearity. It was calculated and is expressed in Eq. 4.16.

$$u = \frac{0.0001 \times 10^{-3}}{\sqrt{3}} = 5.77 \times 10^{-8}\text{Kg} \qquad (4.16)$$

4.2.2.1.3.9. Repeatability

Uncertainty associated with repeatability is found to be 0.00028×10^{-3} kg.

4.2.2.1.3.10. Computation of relative uncertainty due to sample mass

Uncertainty due to sample mass u(m_{sample}) was calculated as shown in Eq. 4.17.

$$u(\mathrm{m_{sample}}) = \sqrt{2 \times (5.77 \times 10^{-8})^2 + (0.00028 \times 10^{-3})^2} = 2.91 \times 10^{-7}\ \text{Kg} \qquad (4.17)$$

From the values of Eq. 4.17 the relative uncertainty due to sample mass in tablet, cream, eye ointment and injection was calculated and found to be 2.90×10^{-2}, 2.93×10^{-2}, 2.94×10^{-2} and 2.93×10^{-2} resp.

4.2.2.1.3.11. Uncertainty due to recovery of method

Results of recovery are evaluated as percentage recovery from sample matrix of representative spiking. The value of recovery was obtained from validation of method as discussed earlier. When a 'spike' is used to estimate recovery, the recovery of analyte from

the sample may differ from recovery of spike so that an uncertainty needs to be evaluated. It was evaluated as Eq. 4.2 and U(C_{spike}) is calculated by using Eq. 4.18 and results of uncertainty due to spiking concentration of standard are represented in Table 4.14.

$$U\ (Cspike) = Cspike\ \times \sqrt{\frac{U(Cbal)^2}{(Cbal)^2} + \frac{U(v)^2}{(v)^2}} \qquad (4.18)$$

Therefore, the standard relative uncertainty of method recovery was calculated using uncertainty due to mass of ACV (from balance), calibration of pipette, calibration of flask and temperature effect, which was found to be 1.97×10^{-7}, 0.0058, 0.0029 and 0.0048 respectively. Combined uncertainty due to these factors was found to be U(v) = 0.00805 mL. Now using the Eq. 4.3 the standard relative uncertainty due to recovery of method was calculated and the results are represented in Table 4.14 for different formulations.

4.2.2.1.3.12. Uncertainty due to precision

Method validation results show the repeatability for determination of ACV in terms of percentage RSD (0.335). This equation can be used directly for calculation of CSU.

U(Rep) = RSD

U(Rep) = 0.00335

4.2.2.1.3.13. Combined standard uncertainty (CSU)

The values of all the parameters having effect on ACV determination are compiled up in Table 4.14 for tablet, skin cream, eye ointment and injection respectively.

These values were further used to calculate ACV quantity by using Eq. 4.1 and thus, we obtained a quantity of 4.06×10^{-5}, 4.00×10^{-5}, 4.06×10^{-5} and 4.07×10^{-5} mol/kg for tablet, skin cream, eye ointment and injection respectively.

The CSU is calculated according to Eq. 4.19

$$\frac{u(\mathrm{ACV_{sample}})}{ACV_{\mathrm{sample}}} = \sqrt{\left(\frac{u(V_{10})}{V_{10}}\right)^2 + \left(\frac{u(\mathrm{C_{10}})}{\mathrm{C_{10}}}\right)^2 + \left(\frac{u(\mathrm{m_{sample}})}{\mathrm{m_{sample}}}\right)^2 + \left(\frac{u(Rm)}{Rm}\right)^2 + \left(\frac{u(Rep)}{Rep}\right)^2} \quad (4.19)$$

$$u\ (ACV_{sample})^{\ tablet} = 2.09 \times 10^{-6}\ mol/kg$$

$$u\ (ACV_{sample})^{\ skin} = 2.10 \times 10^{-6}\ mol/kg$$

$$u\ (ACV_{sample})^{\ ointment} = 2.06 \times 10^{-6}\ mol/kg$$

$$u\ (ACV_{sample})^{\ injection} = 2.09 \times 10^{-6}\ mol/kg$$

4.2.2.1.3.14 Expanded standard uncertainty (EU)

Expanded uncertainty of ACV in different sample matrices was obtained by multiplying the combined standard uncertainty by coverage factor, k = 2, at confidence level of 95%, and, the EU (ACV_{sample}) is as shown

$$EU\ (ACV_{sample})^{\ tab} = 4.17 \times 10^{-6}\ mol/kg$$

$$EU\ (ACV_{sample})^{\ skin} = 4.20 \times 10^{-6}\ mol/kg$$

$$EU\ (ACV_{sample})^{\ ointment} = 4.12 \times 10^{-6}\ mol/kg$$

$$EU\ (ACV_{sample})^{\ injection} = 4.17 \times 10^{-6}\ mol/kg$$

The contribution of different parameters in uncertainty is shown individually for different sample matrices in Figure 4.11.

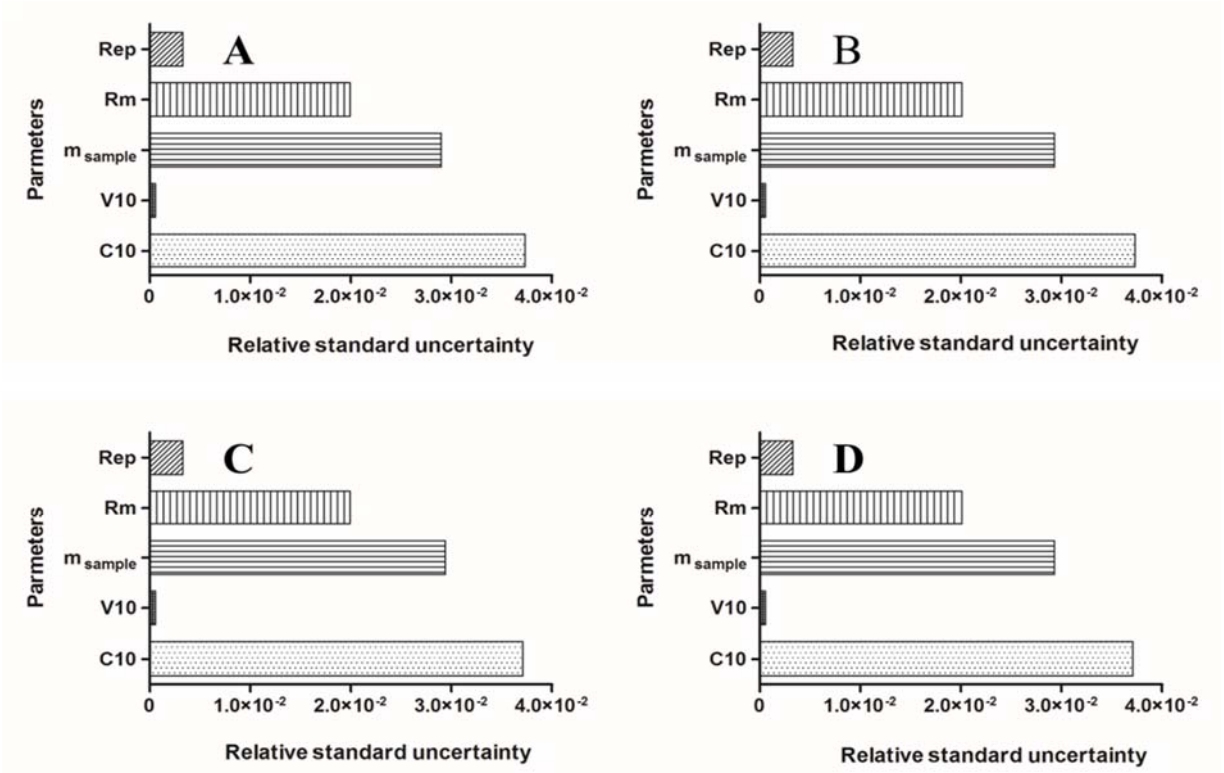

Figure 4.11 Uncertainty profile for acyclovir determination in A) tablets B) skin cream C) eye ointment D) injection representing different components contributing in overall uncertainty and showing maximum effect due to concentration of sample.

Table 4.14 Summary of contribution to the measurement uncertainty

Formulation	Parameter	Volume, V_{10} (mL)	Sample conc. C_{10} (M)	Mass sample, m_{sample} (kg)	Recovery method	Repeatability
Tablet	*Value*	10	4.058×10^{-8}	1.003×10^{-5}	99.63×10^{-2}	-----
	Standard uncertainty, u(x)	5.76×10^{-3}	1.15×10^{-9}	2.91×10^{-7}	1.98×10^{-2}	3.30×10^{-3}
	RSU, u(x)/x*	5.76×10^{-4}	3.73×10^{-2}	2.9×10^{-2}	1.99×10^{-2}	3.30×10^{-3}
	Value	10	4.01×10^{-8}	9.91×10^{-6}	99.75×10^{-2}	-----
Eye Ointment	*Standard uncertainty, u(x)*	5.76×10^{-3}	1.49×10^{-9}	2.91×10^{-7}	1.98×10^{-2}	3.3×10^{-3}
	RSU, u(x)/x*	5.76×10^{-4}	3.71×10^{-2}	2.94×10^{-2}	1.99×10^{-2}	3.3×10^{-3}
	Value	10	4.02×10^{-8}	9.95×10^{-6}	10.10×10^{-1}	-----
Skin Cream	*Standard uncertainty, u(x)*	5.76×10^{-3}	1.49×10^{-9}	2.91×10^{-7}	2.03×10^{-2}	3.30×10^{-3}
	RSU, u(x)/x*	5.76×10^{-4}	3.71×10^{-2}	2.93×10^{-2}	2.01×10^{-2}	3.30×10^{-3}
	Value	10	4.03×10^{-8}	9.96×10^{-6}	99.50×10^{-2}	-----
Injection	*Standard uncertainty, u(x)*	5.76×10^{-3}	1.50×10^{-9}	2.91×10^{-7}	2.0×10^{-2}	3.30×10^{-3}
	RSU, u(x)/x*	5.76×10^{-4}	3.73×10^{-2}	2.93×10^{-2}	2.01×10^{-2}	3.30×10^{-3}

4.2.2.1. LC-MS method for cell line and plasma samples

4.2.2.1.1. Method Development and Optimization

Optimization of the chromatographic conditions is the most critical step having a very specific aim to achieve symmetrical peak shapes with short chromatographic analysis time also having high sensitivity and selectivity. During the optimization higher responding signals and less interference of sample matrix endogenous substances were observed in negative ion mode than positive ion mode by comparing the obtained chromatograms. Thus, negative ion mode was chosen. Ion transitions at m/z 226.0 for ACV were selected for quantification. The CE, DP, CXP, and EP for ACV were optimized to obtain the greater intensity of the target ion pairs. The CE of 40 and 25, DP of 150 and 100, CXP of 10, and 13 and EP of 11 and 11 for ACV were adopted, respectively.

4.2.2.1.2. Validation parameters

In the proposed method calibration curves from the response of different concentration were prepared using linear regression model. The four different sets were prepared for response function studies with range of ACV from 50-1600 ng/mL, from their regression analysis studies series 3, shows the best results with coefficient of determination (r^2) 0.9997, so this series was selected for further computation for validation and sample analysis. Moreover, the selected series and regression model was diagnosed and confirmed using Lack of Fit (LOF) test. The p-values were calculated and found to be greater than 0.05, as illustrated in Table 4.15 and further to demonstrate that no outliers were found in calibration curve standard residual plot were also plotted as represented in Figure 4.12. As the model was established, now in order to authenticate the regression equation back calculation was done and linear plot using absolute β-expectation limit was constructed

between nominal and back calculated concentration which showing the r^2 0.9998 and confirming the authenticity of regression equation.

Table 4.15 Results of LOF for linear regression model

		SS	df	MS	Fcalc	Fcrit,95%	p-value
Lack of Fit test	LOF	7791	8	973.9	1.058	2.849	0.4486
	Error						
	Pure Error	1.1043×10^4	12	920.3			

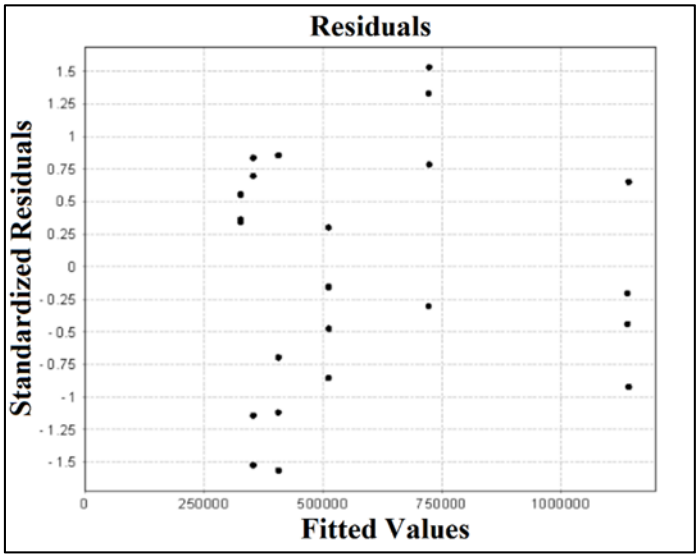

Figure 4.12 Standard residual plot of representing absence of outliers at different concentration levels.

Trueness of method was justified by calculation of %age relative bias which was found to be limited between [-0.03524% -- 0.3887%] as illustrated in Table 4.16 from which it has been concluded that trueness of method is adequate. The method precision and reproducibility was authenticated by results obtained from precision studies which were found to be < 2% in terms of RSD for both repeatability and intermediate levels as illustrated with 95% confidence upper limit in Table 4.17. After the conformation of

accuracy of all the parameters related to system and developed method, sample matrixes was incorporated in validation process which includes recovery studies. Recovery studies were carried out using standard addition method in sample matrixes. These recovery studies receipts into account total error of test results and is represented by the β-expectation tolerance limits. The results of accuracy studies has been illustrated in Table 4.18. The β-expectation tolerance limits was also found to be in the acceptance as accuracy profile illustrated in Figure 4.13. Further, these recovery studies of the method was justified by plotting risk profile keeping maximum risk level at 5.0% from which it was concluded that risk of outliers are within limits and in future analysis of the samples using this developed and validated method will fall within range. The results of LOD show that this method is sensitive enough to analyze the marketed formulations and cell line samples, LOD was found to be 0.189 ng/mL resp.

Table 4.16 Results of Trueness in terms of relative bias (%)

Nominal concentration (ng/mL)	Back calculated concentration (ng/mL)	Absolute bias (ng/mL)	Relative bias (%)
50.00	50.19	0.1943	0.3887
100.00	99.82	-0.1753	-0.1753
200.00	199.5	-0.5356	-0.2678
400.00	399.6	-0.3630	-0.0908
800.00	801.4	1.443	0.1804
1600.00	1599	-0.5638	0.0352

Table 4.17 Results of relative and absolute intermediate precision and repeatability in terms of (%RSD)

	Relative intermediate precision and repeatability				Absolute intermediate precision and repeatability
			95% Upper Confidence Limit		
Nominal Conc (ng/mL)	Rep* (%RSD)	Intermediate precision (%RSD)	Rep* (SD) (ng/mL)	Rep* (SD) (ng/mL)	Intermediate precision* (SD)(ng/mL)
50.00	0.0078	0.1088	0.0172	0.0039	0.0544
100.00	0.7499	0.8267	2.1901	0.7356	0.7259
200.00	0.4559	0.9245	0.3919	0.9117	0.9117
400.00	0.1527	0.3867	2.1690	0.6108	0.9916
800.00	0.1788	0.1239	1.9862	1.4304	1.849
1600.0	0.1032	0.3249	0.2609	1.6524	0.8532

Table 4.18 Result of method accuracy in terms of relative beta-expectation tolerance limit and risk assessment obtained by selected regression model in matrix

	Concentration Level (%)	Concentration (ng/mL)	Beta-expectation tolerance limits (ng/mL)	Relative Beta-expectation tolerance limits (%)	Risk (%)
Tablet	80.0	80.00	[78.29 , 81.71]	[-2.138 , 2.140]	0.1998
	100.0	100.00	[98.55 , 101.4]	[-1.446 , 1.448]	0.0349
	120.0	120.00	[117.9 , 122.1]	[-1.723 , 1.724]	0.07719

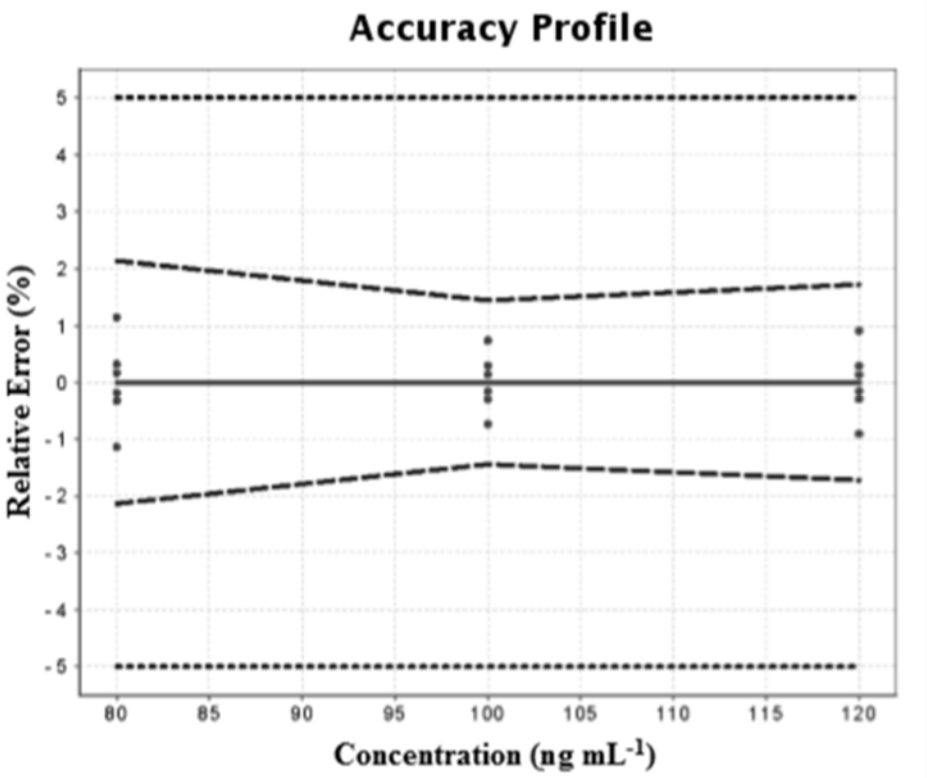

Figure 4.13 Accuracy profile of ACV obtained after application of linear regression using calibration standards prepared with the matrix. The plain line is the relative bias, the dashed lines are the 95% β-expectation tolerance limits and the dotted curves represent the acceptance limits (±5%). The dots represent the relative back-calculated concentrations of the validation standards.

4.2.2.1.3. Application of the developed method to cell line and Plasma samples

4.2.2.1.3.1. Extraction efficiency Cell line samples

Extraction efficiency of the developed method was calculated for cell line samples and was found to be in the range of 95-102%. These results justifies the use of developed method for the analysis of cell line samples.

4.2.2.1.3.2. Extraction efficiency Plasma samples

Extraction efficiency of the developed method was calculated for Plasma samples and was found to be in the range of 89-95%. These results justifies the use of developed method for the analysis of Plasma samples. Results of extraction of ACV from plasma samples has been shown in Table 4.19.

Table 4.19 Extraction efficiency results for plasma samples

	Plasma samples		
Spiked Concentrations (ng/ml)	100	200	400
Mean Observed Concentration (ng/ml)	93.48 ± 2.13	187.34 ± 3.73	377.39 ± 6.49
Mean Extraction (%)	92.40 ± 2.13	92.61 ± 1.86	93.41 ± 1.62
Average Extraction (%)		92.18	

4.2.2.1.4. Measurement of uncertainty

Once uncertainty sources has been identified, they were evaluated and their magnitude was determined. In order to assure the traceability for uncertainty results all the computations were done in International System of Units as concentration in M and weight in kg.

4.2.2.1.4.1. Uncertainty of volumetric flask

The uncertainty due to volumetric flask is mainly influenced by the three parameters i.e. calibration of the volumetric flask at the time of manufacturing, repeatability and temperature.

4.2.2.1.4.2. Calibration of volumetric flask

Deviance from nominal volume of 10 mL volumetric flask is ± 0.006 mL (at 27°C) as given by manufacturer. Standard value of uncertainty can be calculated with triangular distribution. So, uncertainty related to the liberation of volume by volumetric flask (u (V_{10}cal)) is 0.0024.

4.2.2.1.4.3. Repeatability, u (V_{10}rep)

In experiment repeatedly weighing and filling of volumetric flask standard uncertainty established was 0.0016 mL.

4.2.2.1.4.4. Temperature

The manufacturer has calibrated volumetric flask at time of manufacturing at temperature of 27°C, while temperature at laboratory varied with $\Delta t = \pm 4$ °C. This difference can be overcome by calculating uncertainty value with estimation of temperature range and volume dilatation coefficient. Volume expansion of liquid was taken into consideration as it is quite higher than expansion of volumetric flask. The volume expansion coefficient, λ, of water is 2.1×10^{-4} /°C. Uncertainty for 10 mL volumetric flask ΔV_{10} was calculated by Eq 4.9. Thus, we obtain uncertainty for volumetric flask of 10 mL is 0.0084 mL, standard uncertainty due to temperature on liberation of volumetric flask was found to be 0.0048 mL.

4.2.2.1.4.5. Uncertainty associated with the sample mass m_{sample}

Sample mass has three types of uncertainty sources sensitivity, linearity, and repeatability. Mass of the sample was expressed in kg to convince traceability of results.

4.2.2.1.4.6. Sensitivity

The difference in weighed mass was in very less range and it was measured on the same weighing balance. Thus uncertainty due to sensitivity of balance can be neglected.

4.2.2.1.4.7. Linearity

A rectangular distribution was assumed to convert contribution of linearity. It was calculated as using Eq. 4.13.

4.2.2.1.4.8. Repeatability

Uncertainty associated with repeatability is found to be 2.08 x 10^{-7}kg.

4.2.2.1.4.9. Computation of relative uncertainty due to sample mass

Using the uncertainty due to linearity and repeatability the uncertainty due to sample mass u (m_{sample}) was calculated using Eq. 4.17 was found to be 2.25×10^{-7} Kg

4.2.2.1.4.10. Uncertainty associated with Concentration, (C_{10})

Analytical responses were collected after each injection of standard solution of different concentrations. These responses were used to construct calibration curve. Regression equation of calibration curve was identified such as, slope 8.66 x 10^{13} and intercept 342014.34. Uncertainty involved in the construction of calibration curve was estimated by injecting 6 different concentration solutions each measured three times and sample solution was measured ten times from which Sr and Sxx values were computed as shown in Eq 4.4, which were further used to calculate standard relative uncertainty, due to concentration.

$$Sxx = 3.47 \times 10^{-17}$$

$$Sr = 273.03$$

4.2.2.1.4.11. Uncertainty due to recovery of method

Results of recovery are evaluated as percentage recovery from sample matrix after spiking a known amount. When term 'spike' is used to estimate recovery, the recovery of analyte from the sample may differ from recovery of spike so that an uncertainty needs to be evaluated. Uncertainty due to spiking is found to be 8.76 x 10^{-10}. Standard relative uncertainty of method recovery was calculated using uncertainty due to mass of ACV (from balance), calibration of pipette, calibration of flask and temperature effect, which was found to be 1.98 x 10^{-5}, 0.0052, 0.0029 and 0.0048 respectively. Combined uncertainty due to these factors were found to be U (Rmf) = 1.99.

4.2.2.1.4.12. Uncertainty due to precision

Method validation results show the repeatability for determination of ACV in terms of % age RSD (0.6793). This equation can be used directly for calculation of CSU.

$$U\ (Rep) = RSD$$

$$U\ (Rep) = 0.6793$$

4.2.2.1.5. Combined standard uncertainty (CSU)

The values of all the parameters having effect on ACV determination, these are compiled up in Table 4.20. These values of parameters were further used to calculate ACV quantity by using Equation 1 and thus, we obtained a quantity of 4.17 x 10^{-7}, mol/kg.

4.2.2.1.6. Expanded Standard uncertainty (EU)

Expanded Uncertainty of ACV in sample matrices was obtained by multiplying the combined standard uncertainty by coverage factor k = 2 at confidence level of 95%, and, the EU (ACV_{sample}) is as shown

$$EU\ (ACV_{sample})\ tab = 2.51 \times 10^{-8}\ mol/kg$$

The contribution of different parameters in uncertainty is shown individually for sample matrix has been illustrated in Figure 4.14.

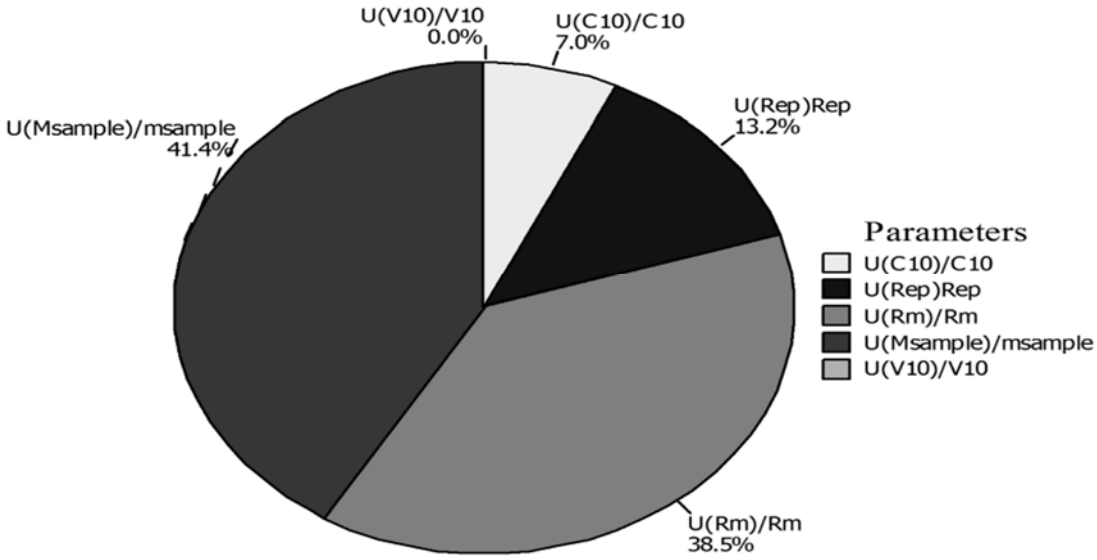

Figure 4.14 Uncertainty profile representing different components contributing in overall uncertainty

Table 4.20 Combine standard uncertainty for LC-MS method

Parameter	Volume, V_{10} (mL)	Sample conc. C_{10} (M)	Mass sample, m_{sample} (kg)	Recovery method	Repeatability
Value	10	4.43×10^{-10}	1.06×10^{-5}	100.20×10^{-2}	-----
Standard uncertainty, u(x)	3.16×10^{-5}	1.60×10^{-12}	2.25×10^{-7}	1.99	6.79×10^{-3}
RSU, u(x)/x*	3.16×10^{-6}	3.60×10^{-3}	2.13×10^{-2}	1.98×10^{-2}	6.79×10^{-3}

4.2.3. Compatibility and uniformity of content studies of binary systems prepared

The prepared mixture were tested for uniformity of content and results were found to be within the range of 99-101%. As shown in Table 4.21.

Table 4.21 Content of Uniformity of different binary systems

Weight Ratio	% ASSAY					
	5:0.5	**5:1**	**5:1.5**	**5:2**	**5:2.5**	**5:3**
ACV-QU	99.85 ± 0.42	99.25 ± 0.66	99.05 ± 0.36	99.18 ± 0.26	100.02 ± 0.35	99.85 ± 0.55
ACV-Sil	100.02 ± 0.88	99.55 ± 0.28	100.06 ± 0.43	99.25 ± 0.35	99.29 ± 0.15	99.62 ± 0.51
ACV-LT	99.05 ± 0.22	99.00 ± 0.12	99.12 ± 0.19	99.14 ± 0.26	100.21 ± 0.58	99.25 ± 0.59

4.2.3.1. Fourier Transform Infrared Spectroscopy (FTIR)

FTIR spectrums of ACV, QU, Sil, LT and ACV:QU, ACV:Sil, ACV:LT binary systems were recorded. The recorded spectrums were interpreted in terms of change in any characteristic peaks of the ACV. The characteristics peaks in the FTIR studies of ACV exhibited an absorption band at about 1723 cm^{-1} due to carboxylic acid functional group and 1^{o} amine of ACV has a strong band at 3309.2 cm^{-1} these characteristic bands confirms the structure of ACV as compared with literature. All these characteristic peaks remains regular in the prepared different binary systems. Although, there was a slight (not significant) change observed in the intensities of the peaks of ACV. These primary results of the FTIR spectra

revealed that there was no physical interaction between ACV, QU, Sil and LT in binary system. It also confirms that there is no interaction at the molecular level in the ACV and their binary system. The FTIR spectrum of ACV and different binary system has been shown in Figure 4.15.

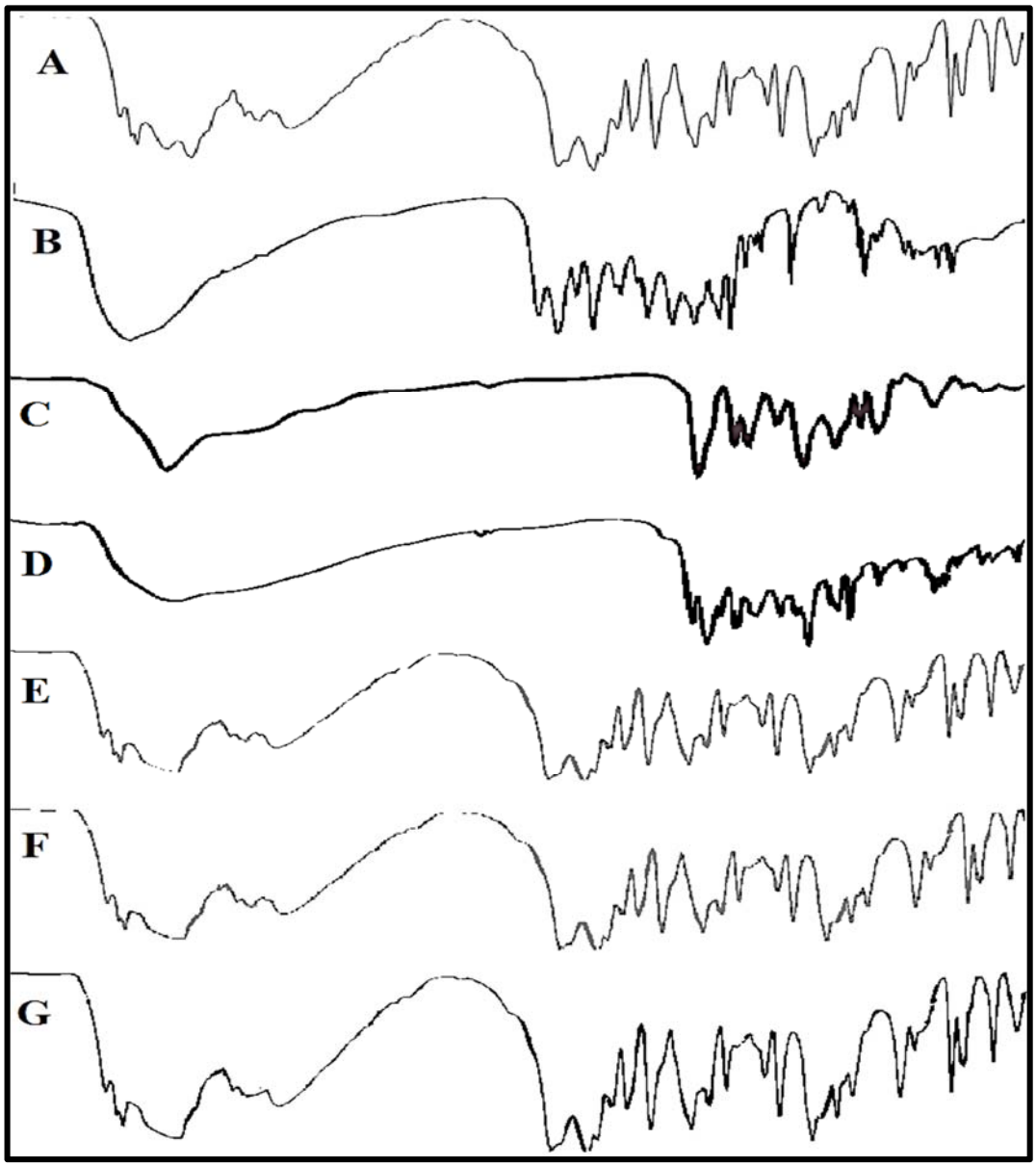

Figure 4.15 FTIR spectrum of (A) ACV (B) QU (C) Sil (D) LT (E) ACV:QU (F) ACV:Sil (G) ACV:LT for compatibility studies.

4.2.3.2. Differential Scanning Calorimetry (DSC)

Differential scanning calorimetry (DSC) thermograms of the ACV, QU, Sil and LT has been recorded. These recorded thermograms were interpretated to know the interactions. Interpretations of the thermograms revealed that there is no physical interaction between the ACV, QU, Sil and LT in their respective binary systems. The DSC thermogram of ACV showed an endothermic peak at 254.53°C which was corresponding to its melting point. While the thermogram of QU shows an endothermic peak at 322°C. Sil shows a broad endothermic peak in the range of 166-173°C. The luteolin thermogram showed endothermic peak on 328.16°C, which again attributed to its melting point. DSC thermogram of ACV:QU physical mixture shows an endothermic peak at 250.32°C which is very near to the pure ACV, which reveals that there is no interaction in the QU and ACV. The DSC thermogram of all the pure compounds and binary mixtures has been illustrated in Figure 4.16.

DSC thermogram of ACV:Sil physical mixture shows an endothermic peak at 249.65°C which is slightly lower than the pure ACV, although it is not significant, the endothermic peak of binary mixture suggest minimal or no physical interaction between the QU and Sil. DSC thermogram of ACV:LT physical mixture shows an endothermic peak at 252.31°C which is at the lower side of the pure ACV, the endothermic peak of ACV:LT binary mixture suggests no physical interaction between the ACV and LT. The DSC data of all the samples encourages and clears the way for the researchers to move further for the permeation studies.

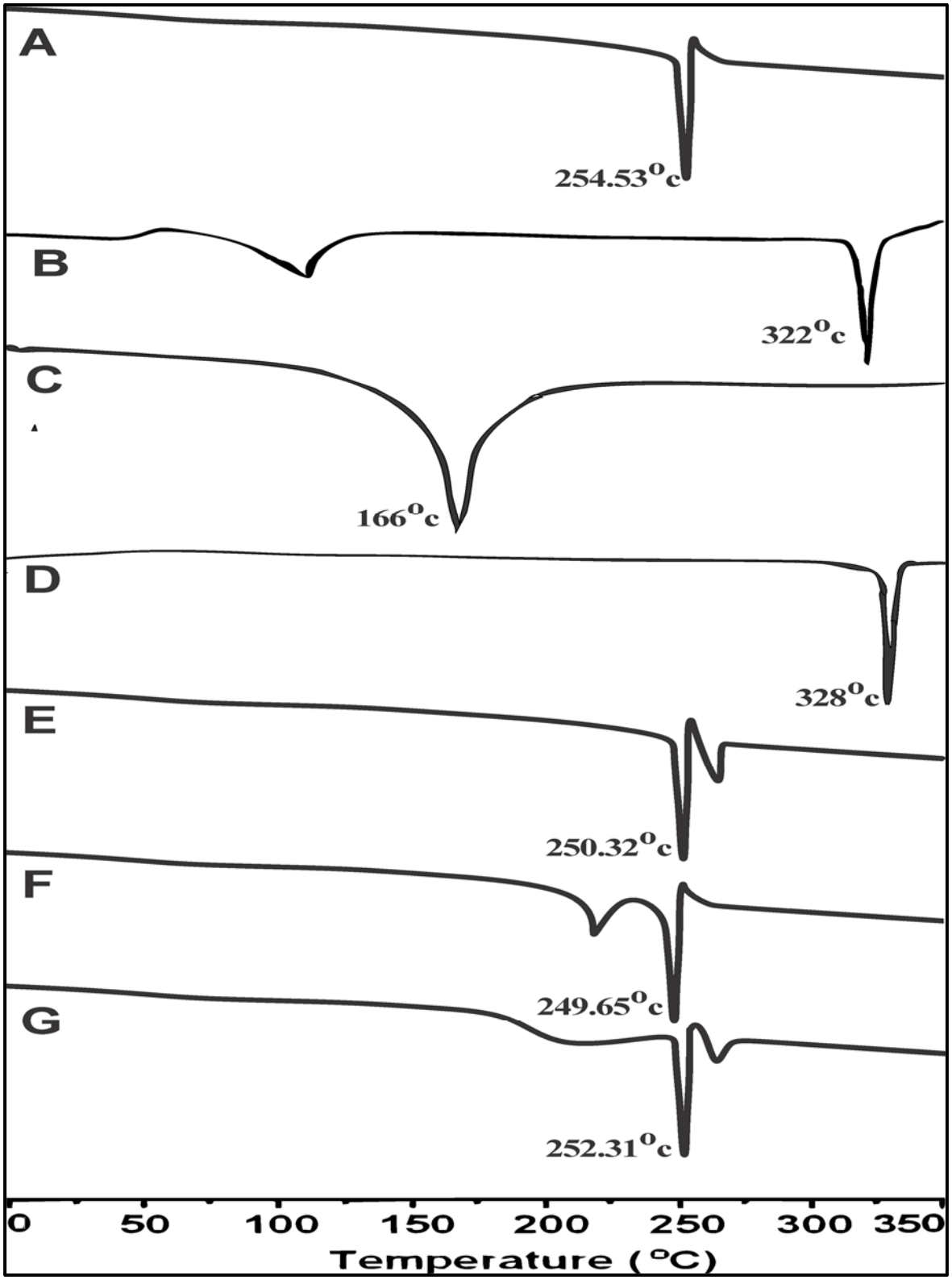

Figure 4.16 DSC thermogram of A) ACV B) QU C) Sil D) LT E) ACV:QU F) ACV:Sil G) ACV:LT

4.2.4. *Ex-vivo* permeation studies

The permeability of binary systems of ACV:QU, ACV:Sil and ACV:LT in intestinal tissue shows a significant rise in the permeation as compared to the plain ACV. Permeation coefficient (P_{eff}) was calculated for ACV and ACV:QU, ACV:Sil and ACV:LT binary systems. The permeation coefficients calculated for the all weight ratios has been summed up in Table 4.22. The permeation coefficient for plain ACV was $(0.435 \pm 0.02) \times 10^{-6}$ cm/s. The QU shows an increase in the amount permeated with having permeation coefficient $(0.675 \pm 0.02) \times 10^{-6}$ cm/s at weight ratios (5:2), while Sil shows maximum permeation coefficient $(0.682 \pm 0.01) \times 10^{-6}$ cm/s at weight ratios (5:1) and LT shows maximum enhancement at weight ratio (5:2.5) with permeation coefficient $(0.621 \pm 0.03) \times 10^{-6}$ cm/s. Release profile of the ACV and ACV:QU binary system with time has been shown in Figure 4.17. It can be clearly observed from the release profile the maximum peremeation enhancement has been founded with the 5:2 weight ratios in ACV:QU binary system followed by 5:1.5 and 5:2.5 ratios. While in ACV:Sil release profile shown in Figure 4.18 it can be clearly concluded that the maximum enhancement has been found with weight ratio 5:1 (ACV:Sil). In the case of ACV:LT the maximum release has been found with the ratio 5:2.5 as clearly shown in Figure 4.19.

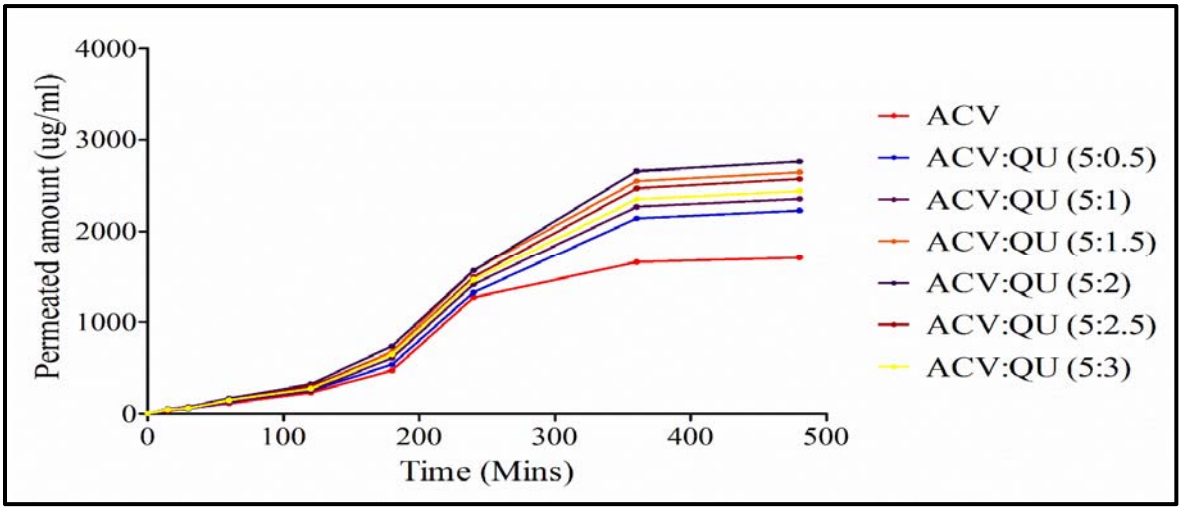

Figure 4.17 Release time profile of the ACV and ACV:QU binary system.

Table 4.22 Permeation coefficient and Enhancement ratio (ER) for ACV and ACV:QU, ACV:Sil, ACV:LT at different weight ratios

Permeation coefficient and enhancement ratio (ER) of ACV and its different binary systems (x 10^{-6} cm/s)

ACV	0.435 ± 0.02					
Weight Ratio	**5:0.5**	**5:1**	**5:1.5**	**5:2**	**5:2.5**	**5:3**
	Peff	**Peff**	**Peff**	**Peff**	**Peff**	**Peff**
ACV-QU	0.534 ± 0.02	0.562 ± 0.01	0.658 ± 0.03	**0.675 ± 0.02**	0.603 ± 0.01	0.588 ± 0.01
ACV-Sil	0.553 ± 0.01	**0.682 ± 0.01**	0.627 ± 0.03	0.523 ± 0.01	0.485 ± 0.01	0.429 ± 0.01
ACV-LT	0.442 ± 0.03	0.457 ± 0.02	0.479 ± 0.02	0.559 ± 0.03	**0.621 ± 0.03**	0.511 ± 0.03
Weight Ratio	**5:0.5**	**5:1**	**5:1.5**	**5:2**	**5:2.5**	**5:3**
	ER	**ER**	**ER**	**ER**	**ER**	**ER**
ACV-QU	1.23	1.29	1.51	**1.55**	1.39	1.35
ACV-Sil	1.27	**1.57**	1.44	1.20	1.11	0.98
ACV-LT	1.02	1.05	1.10	1.28	**1.43**	1.17

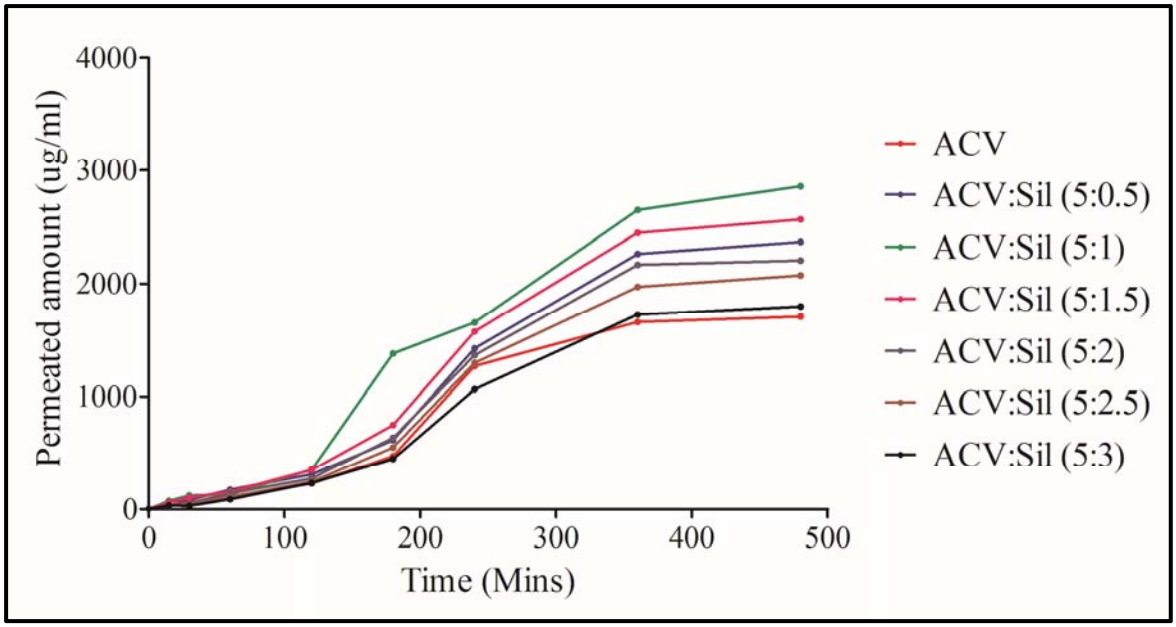

Figure 4.18 Release time profile of the ACV and ACV:Sil binary system

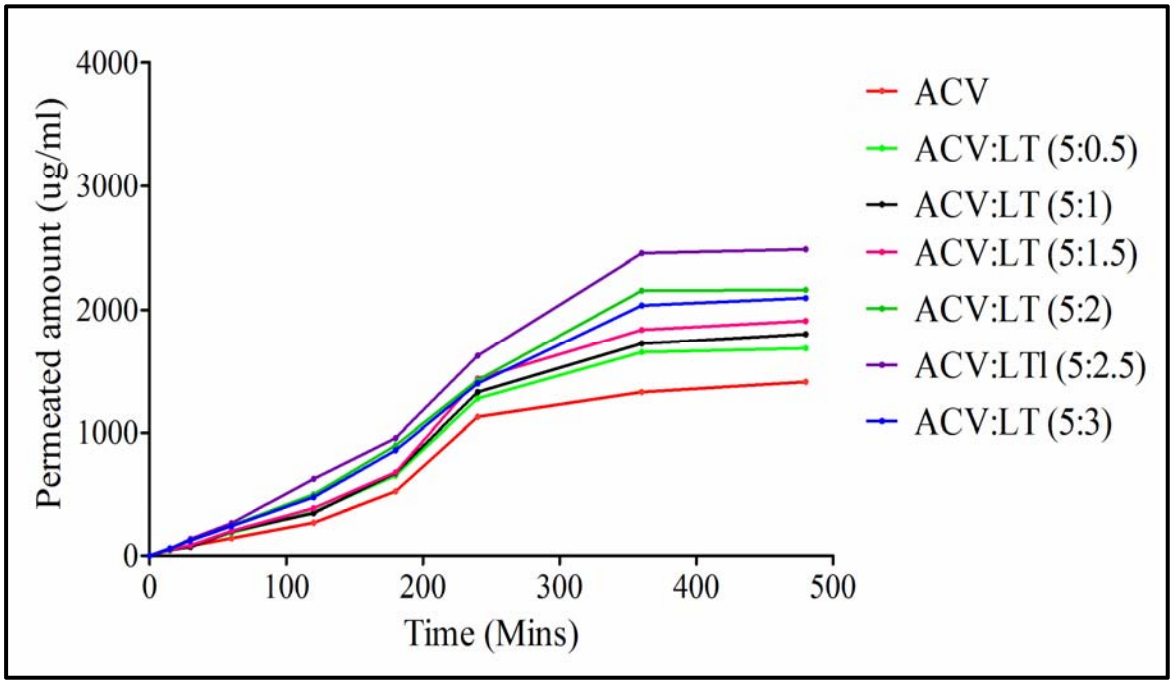

Figure 4.19 Release time profile of the ACV and ACV:LT binary system

4.2.5. Cellular uptake and Transport of ACV across the Caco-2 cell monolayers

Cellular uptake

Cellular uptake of ACV has been shown in Figure 4.20. It can clearly observed from the images that very few individual particles has been seen in the ACV as compare to the binary mixtures. Hence, it shows that there is increase in the uptake of the ACV in presence of the bioenhancers. To know the quantitative effect further transport studies were carried out.

Transport Study

To study the effect of the bioenhancers on ACV transport through cell monolayers, drug transport across Caco-2 cell monolayers from the apical (AP) side to the Basolateral (BL) side were studied. TEER was determined in all the experiments, all the wells used in the experimentation having TEER values above 300 $\Omega \cdot cm^2$ which clearly shows there was no cellular damage. The few wells whose TEER value was less than 300 $\Omega \cdot cm^2$ has been excluded from the studied. As different bioenhancers are having different impact on the cell monolayer so the effect of presence of different concentration of QU, Sil and LT on TEER has been studied. Figure 4.21 shows effect of different concentration of QU, Figure 4.22 and 4.23 shows effect of different concentration of Sil and LT respectively. The effect was studied with considering the pre experimentation value as the 100% and from the observations it has been concluded that the integrity was not rudely affected by the different concentrations of the bioenhancers.

Cell viability

Caco-2 monolayers which are treated with ACV and binary systems shown very similar viability, which further suggests that permeation enhancement was not due to loss of cell viability.

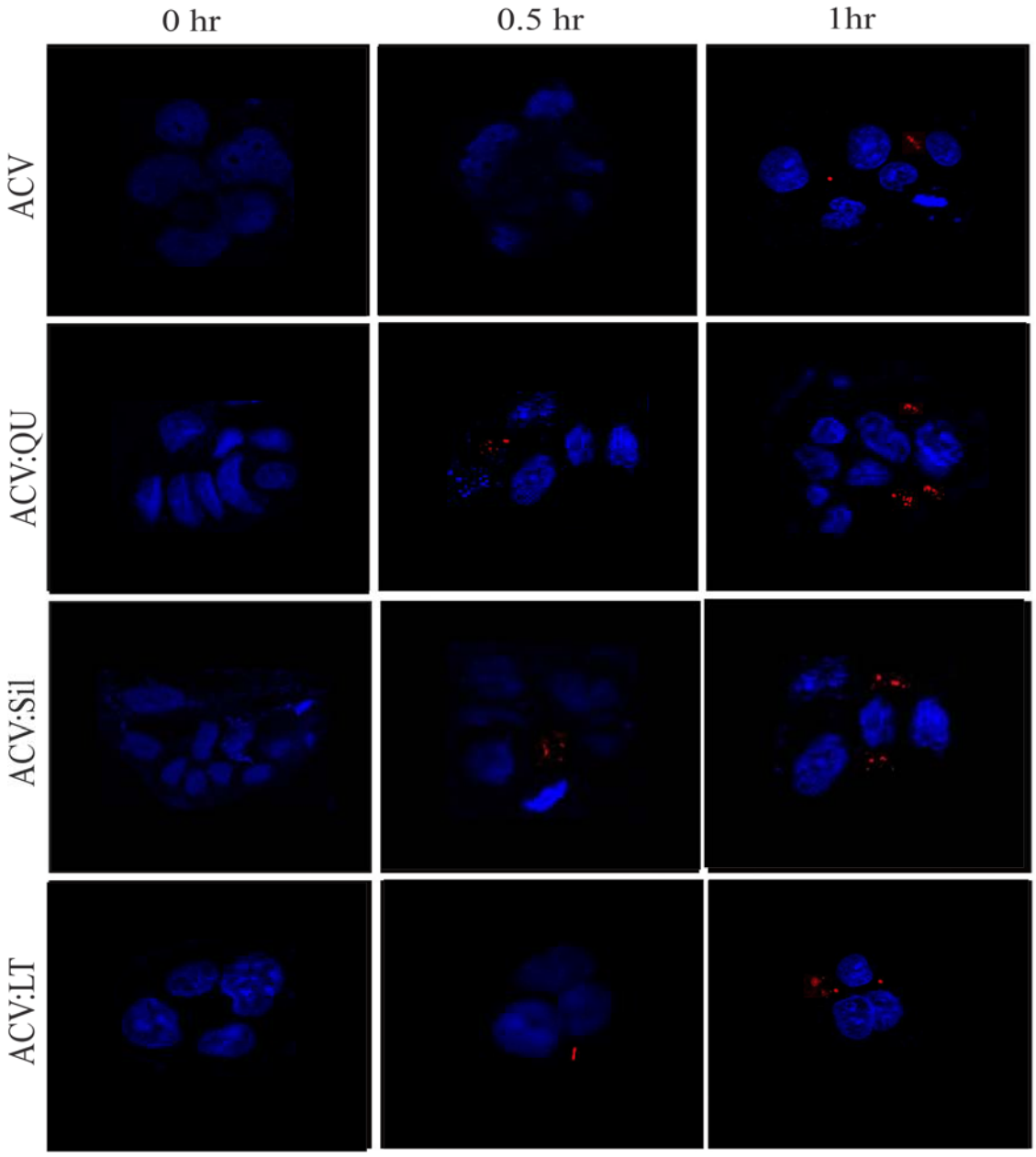

Figure 4.20 Cellular Uptake of ACV and binary system at different time points (0hr, 0.5hr, 1hr)

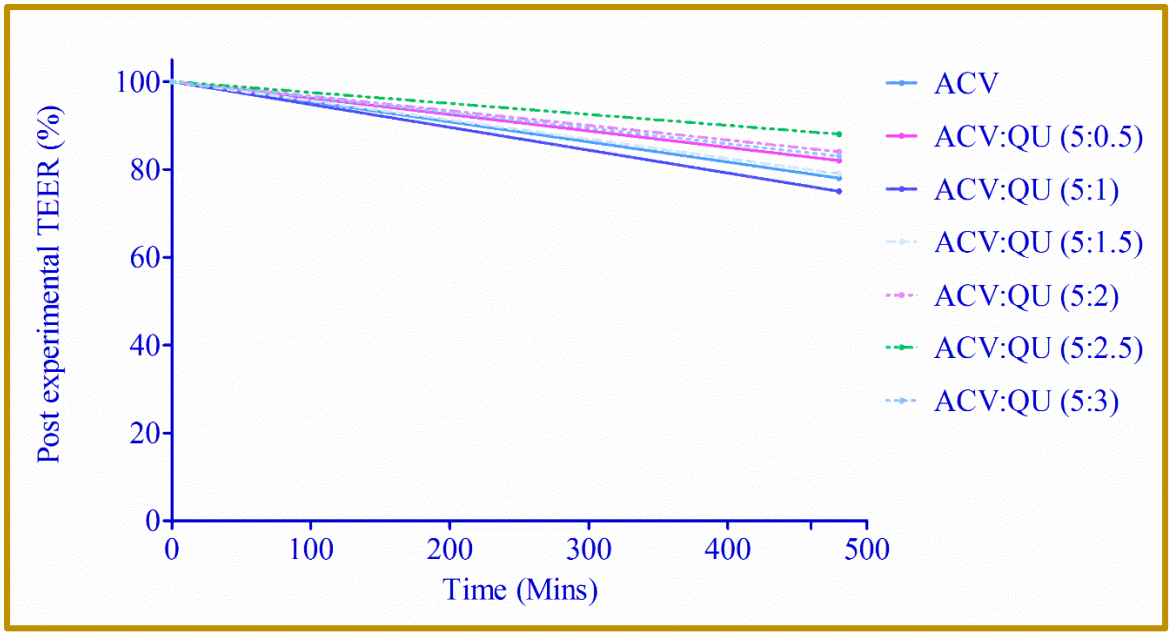

Figure 4.21 Effect of different ratios of Quercetin on TEER Values of Caco-2 cell line

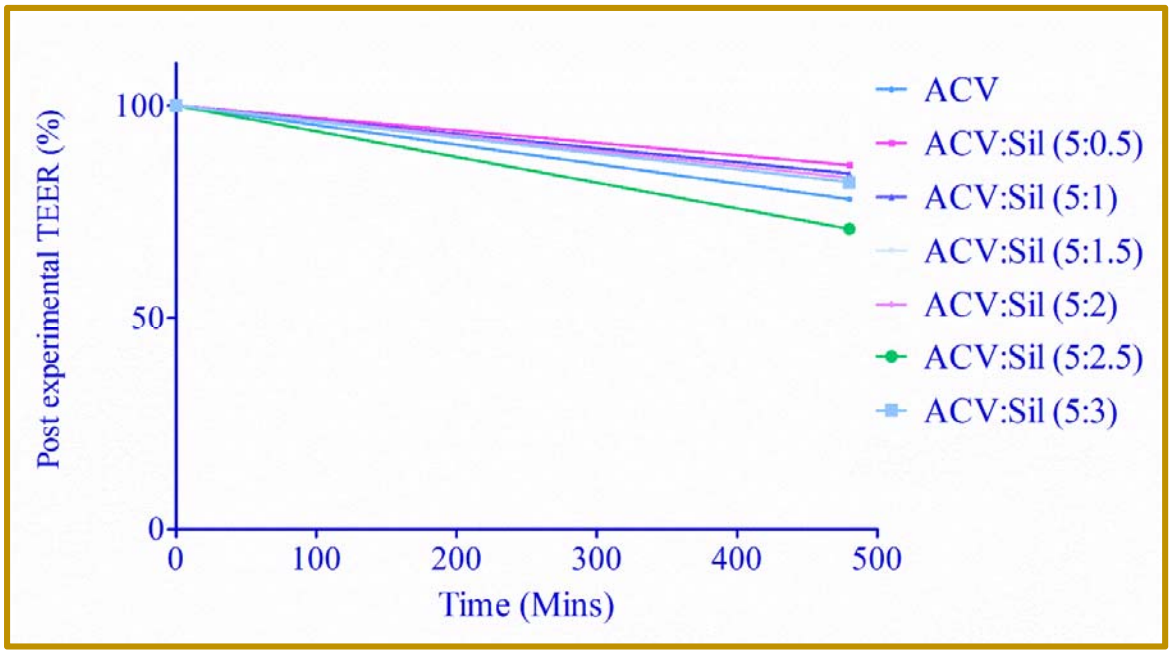

Figure 4.22 Effect of different ratios of Silibinin on TEER Values of Caco-2 cell line

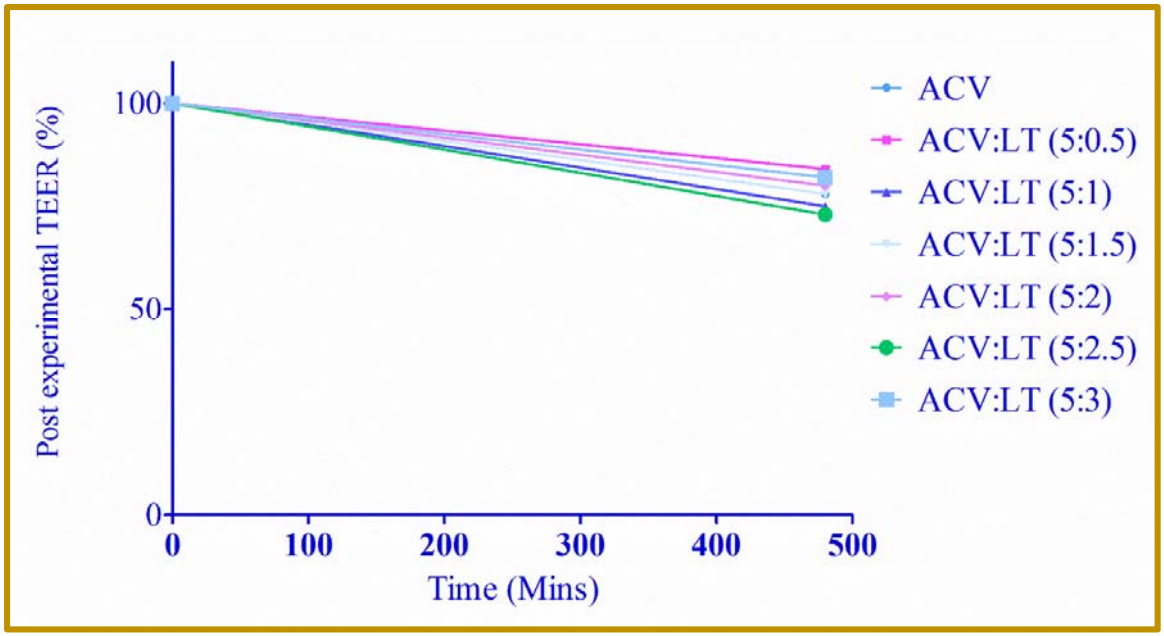

Figure 4.23 Effect of different ratios of Luteolin on TEER Values of Caco-2 cell line

The permeation profile with respect to time of ACV and different binary systems has been shown in Figure 4.24, 4.25 and 4.26 for QU, Sil and LT respectively. In the time permeation release graphs it can be clearly seen that the amount of ACV in the BL side increased with the time for all the samples including binary systems. It is also observed that the concentration in the samples having QU, Sil and LT was higher than the plain ACV.

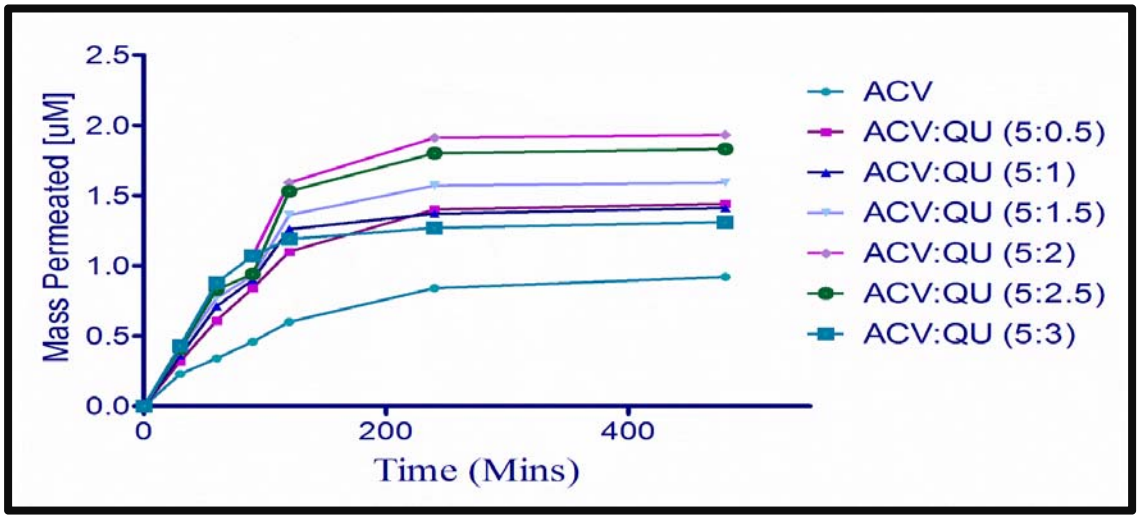

Figure 4.24 Release time profile of ACV and ACV:QU binary system in Caco-2 cell lines

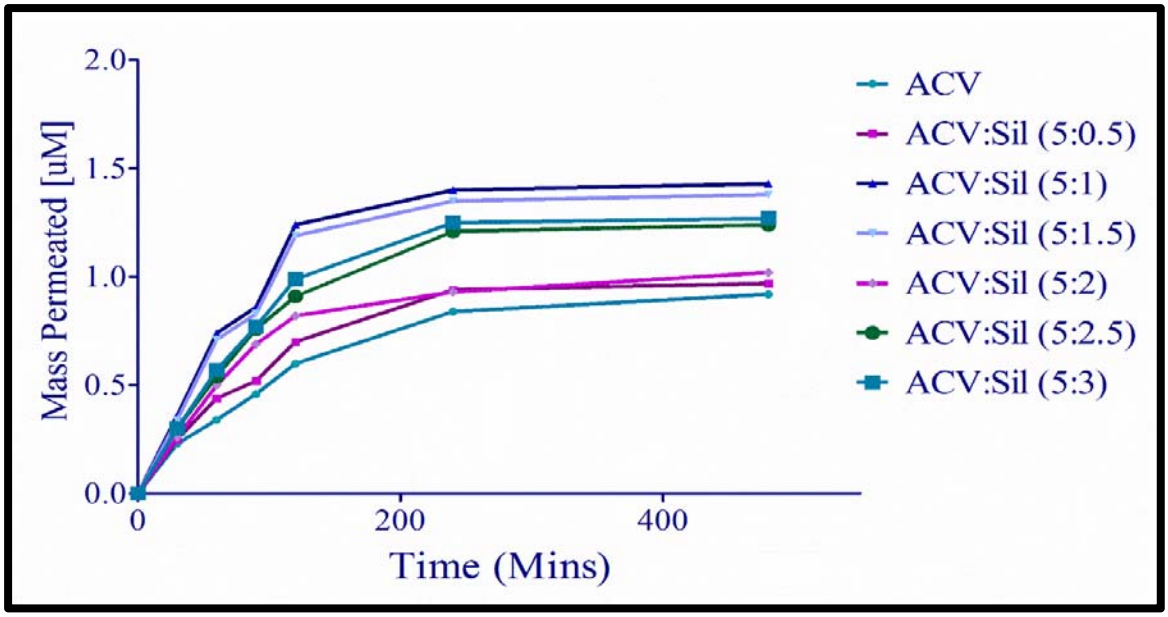

Figure 4.25 Release time profile of ACV and ACV:Sil binary system in Caco-2 cell lines

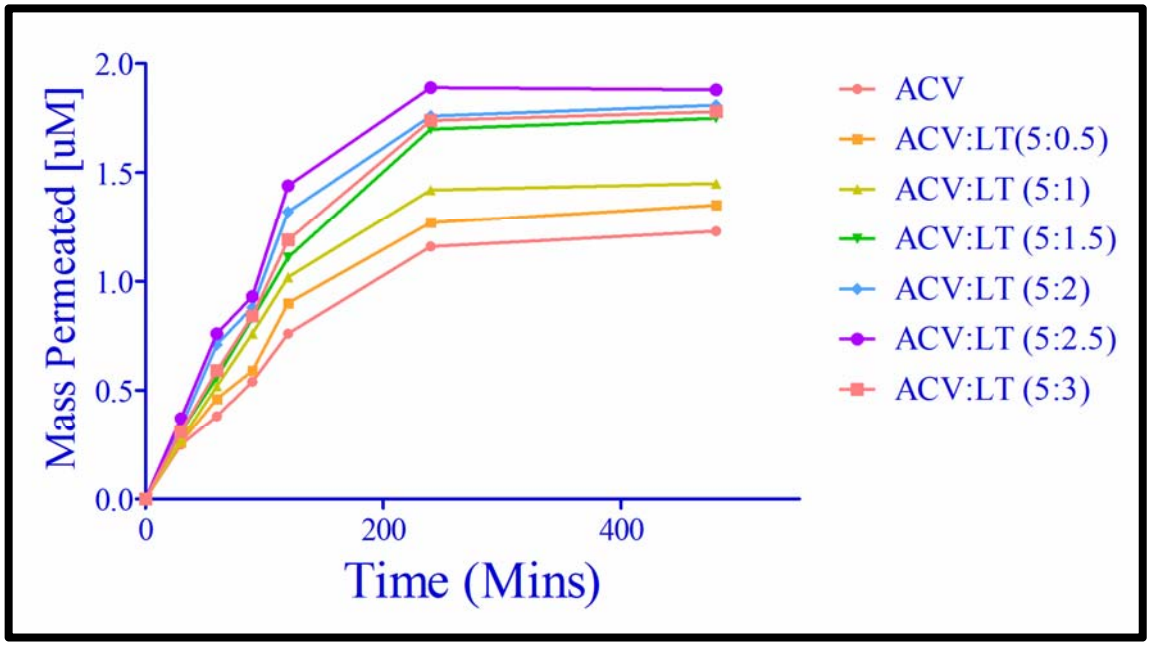

Figure 4.26 Release time profile of the ACV and ACV:LT binary system in Caco-2 cell lines

The *P*app (AP to BL side) of ACV and its binary systems were calculated for 8 hrs. As shown in Figure 4.27, 4.28 and 4.29 maximum *P*app was observed with the QU in the ratio of 5:2 while in the Sil and LT maximum was observed in the ratio of 5:2 and 5:2.5

respectively. Although it was also observed that the ratio of Sil 5:1.5 was very close, but 5:2 concentration also shows maximum enhancement in the ex-vivo studies so this was chosen as optimum concentration for pharmacokinetic studies.

ER comparison chart for the best ratios has been shown in Figure 4.30 was prepared for the best ratios of individual bioenhancers from which it can be easily concluded that the QU shows the maximum ER while the silibinin showing least ER as compared to LT and QU. So from this it can be concluded that the QU can act as the best bioenhancers in combination with the ACV and hence can make a noteworthy change in therapeutic efficacy of the ACV treatment, by increasing its bioavailability. To prove it further these best ratios were then used in *in-vivo* pharmacokinetic studies.

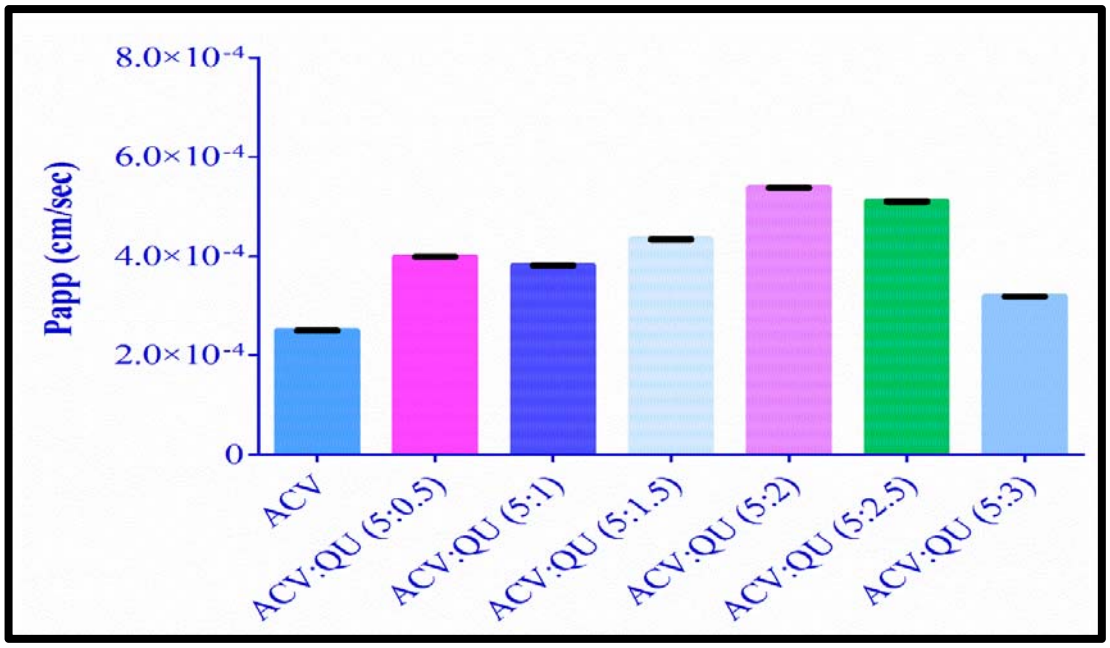

Figure 4.27 Papp comparison of ACV and ACV:QU different weight ratios from AP to BL side

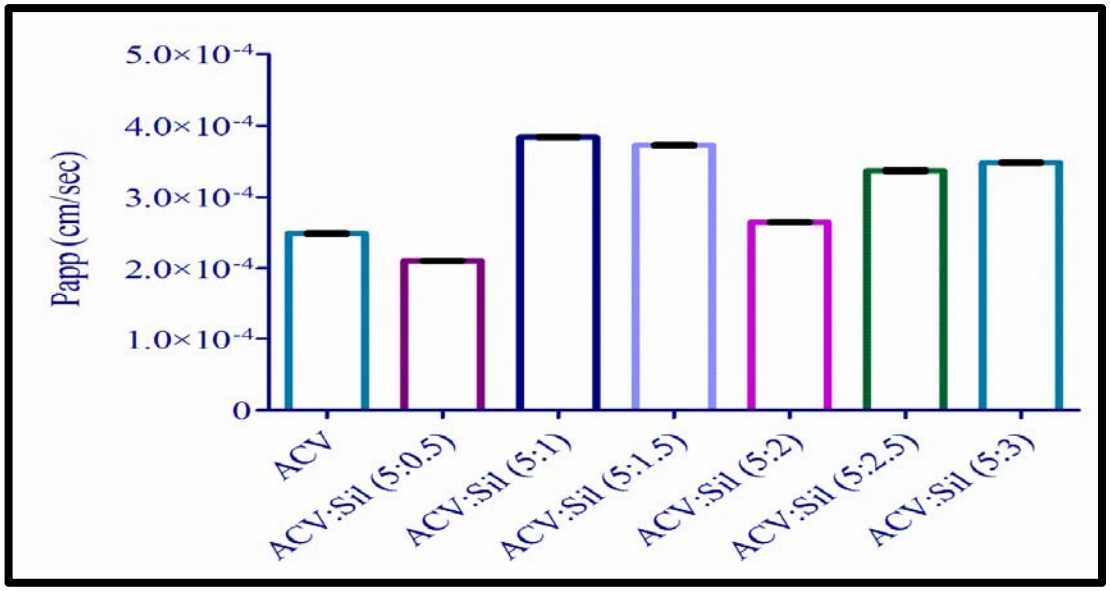

Figure 4.28 Papp comparison of ACV and ACV:Sil different weight ratios from AP to BL side

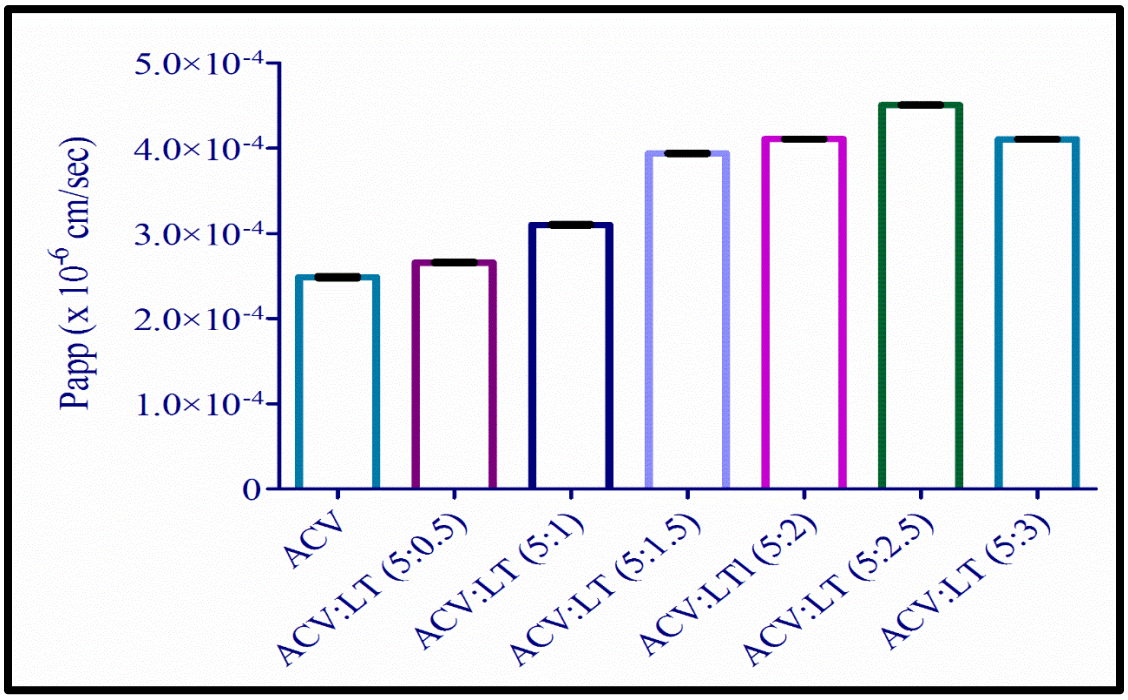

Figure 4.29 Papp comparison of ACV and ACV:LT different weight ratios from AP to BL side

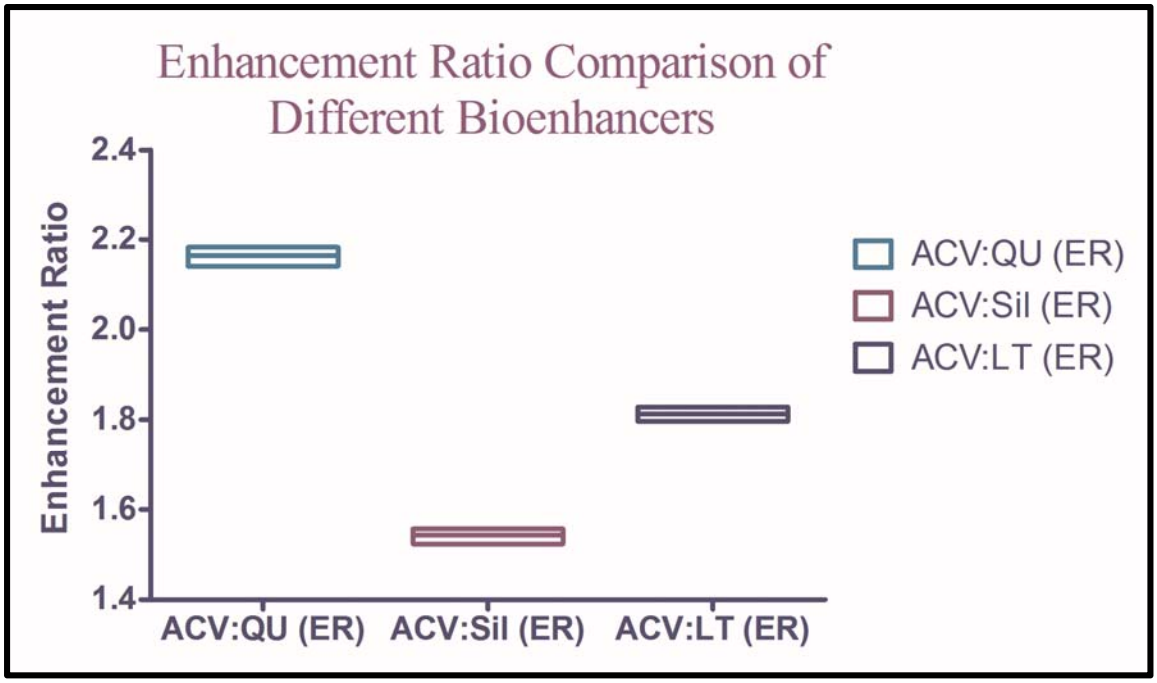

Figure 4.30 Enhancement Ratio (ER) comparison for different bioenhancers with maximum Papp

4.2.6. Pharmacokinetic studies of ACV in rabbits

The pharmacokinetics of ACV were studied in rabbits to evaluate the enhancement in the absorption efficiency of the ACV in combination with QU, Sil and LT. Plasma drug concentration versus time profile and semi log plot for concentration-time profile of ACV and ACV:QU (5:2), ACV:Sil (5:1) and ACV:LT (5:2.5) were plotted as shown in Figure 4.31 & 4.32. After the oral administration of the ACV and binary systems there was significant difference was observed in the pharmacokinetic profile. AUC increase by 4.87 folds in the case of the QU. While, 3.22 and 2.74 folds increase was observed with the Sil and LT respectively. The comparison of ER has been shown in Figure 4.33. Elimination phase, absorption phase composite graphs has been illustrated in Figure 4.34, 4.35, 4.36 and 4.37. The absorption phase is very much similar in all the cases although a small change in the elimination phase has been reported. The pharmacokinetic parameters for all

the three bioenhancers are shown in Table 4.23. The Tmax was found to 1.5 hr for plain ACV, while with the bioenhancers it increases up to 2 hrs. There was an increase in the Cmax when ACV is co-administered with the bioenhancers, which clearly indicates the effectiveness of the bioenhancers. As per ER maximum enhancement was found with the QU as compared to the Sil and LT, the reason for that may be its well established dual activity of inhibiting P-gp and CYP activity, yet need to unfolded by specific studies on CYP enzyme family. bioenhancers enhances the plasma drug concentration approx. 3 folds which clearly shows it effectiveness as a bioenhacer and can be incorporated with the oral dosage form of the ACV for herpes treatment. In the present study results also unfolds the hidden LT as a bioenhancers as its ER is less as compare to other but it shows a significant change in the AUC and Cmax of ACV. So these studies unfold several other research part for researchers as development of dosage form with bioenhancers.

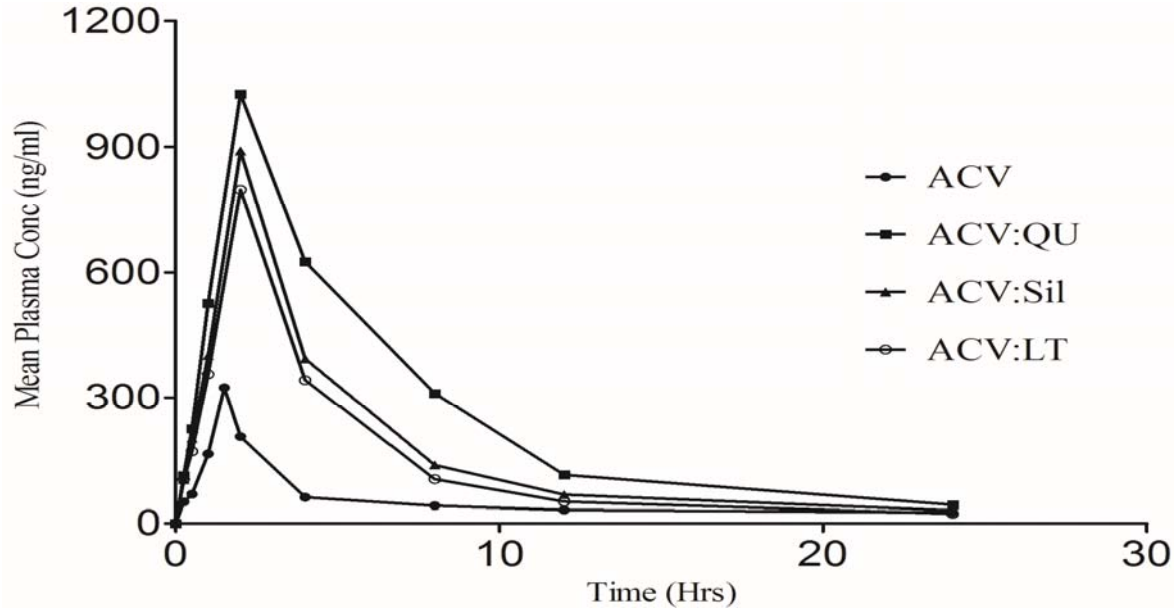

Figure 4.31 Mean Plasma Concentration and Time profile for ACV, ACV:QU, ACV:Sil and ACV:LT

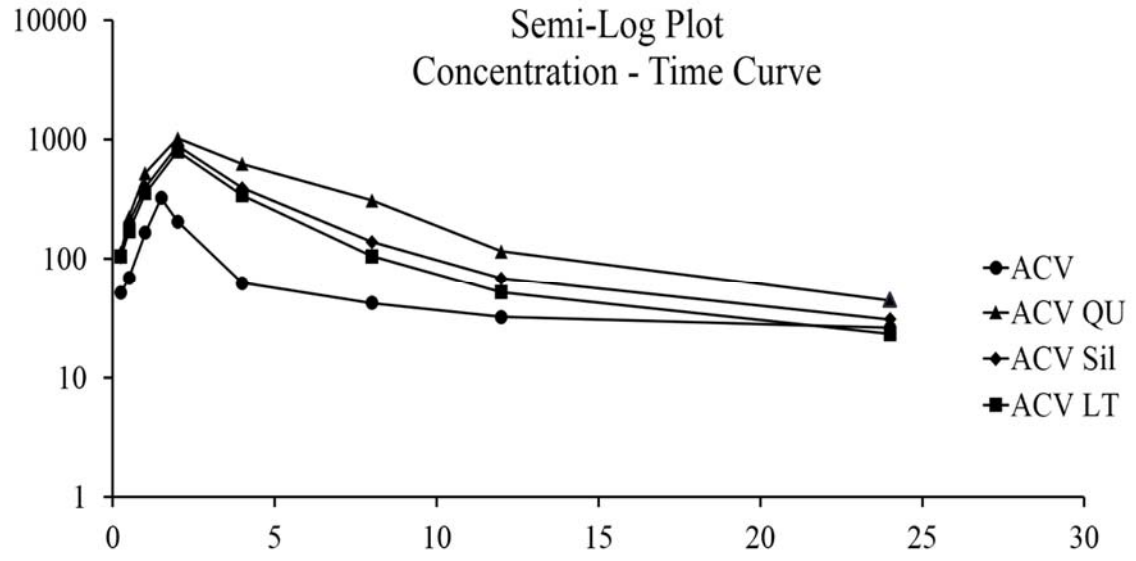

Figure 4.32 Semi Log Plot for Concentration vs Time for ACV, ACV:QU, ACV:Sil, ACV:LT

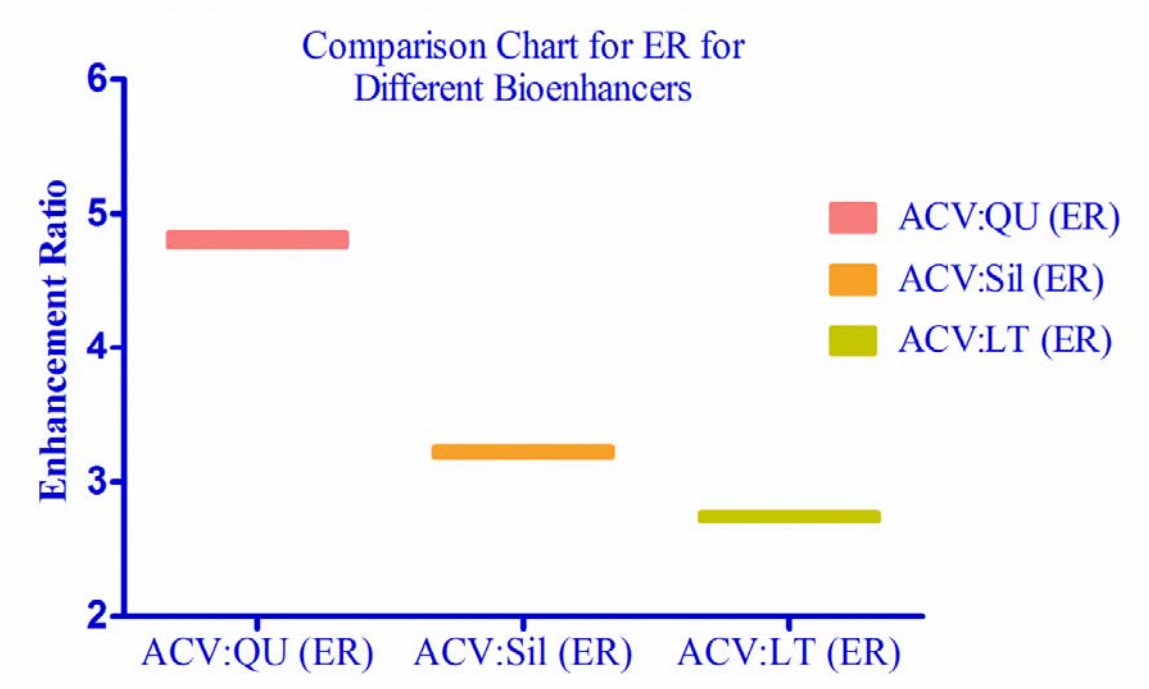

Figure 4.33 Enhancement Ratio (ER) comparison for different bioenhancers with respect to AUC

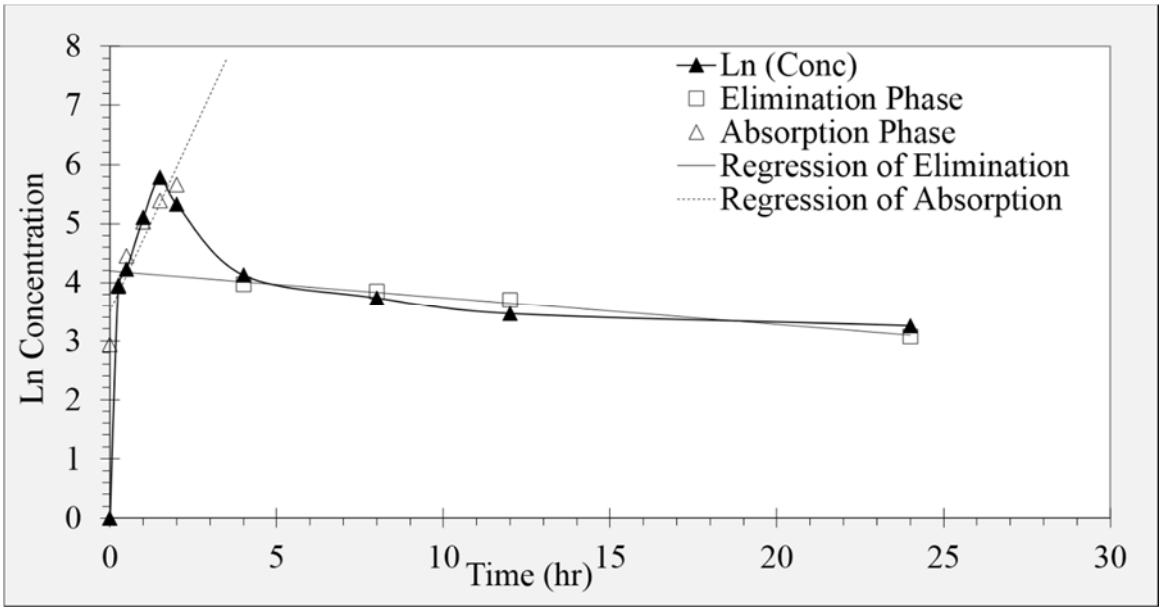

Figure 4.34 Ln concentration time profile including absorption and elimination phase for ACV

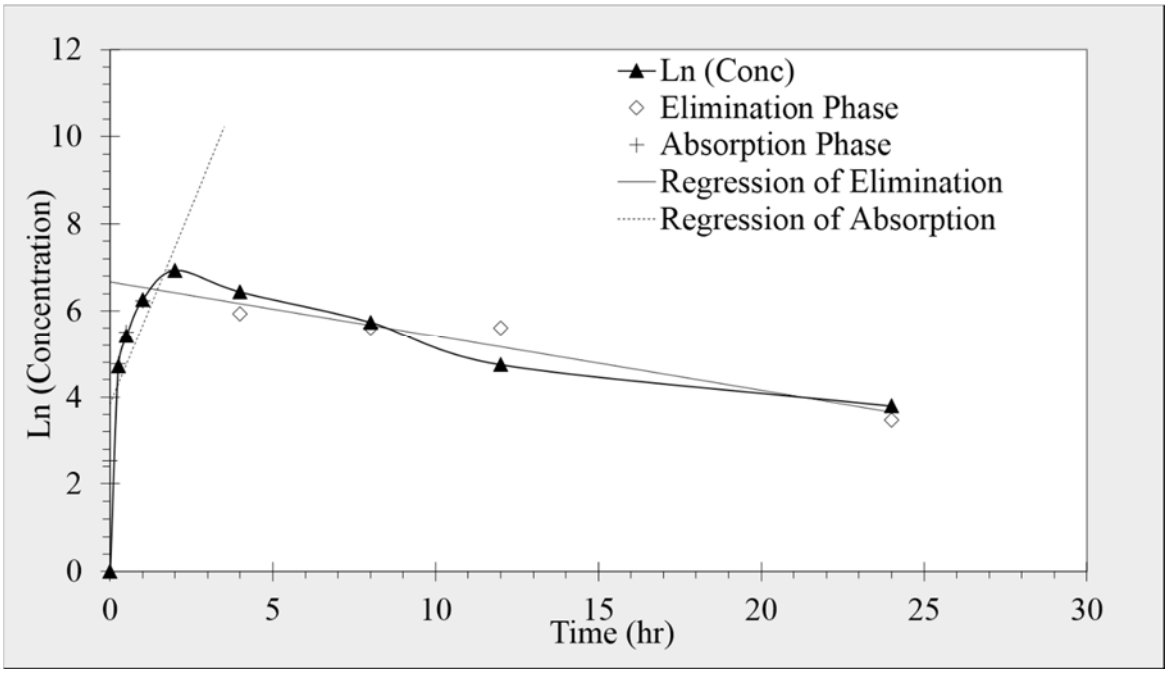

Figure 4.35 Ln concentration time profile including absorption and elimination phase for ACV:QU

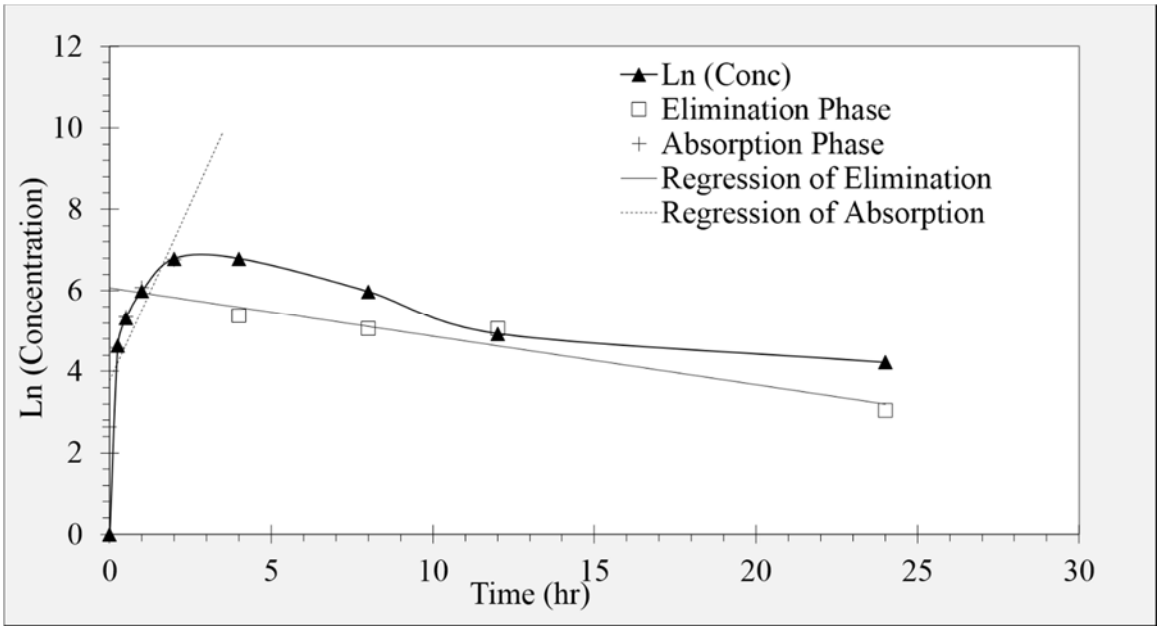

Figure 4.36 Ln concentration time profile including absorption and elimination phase for ACV:Sil

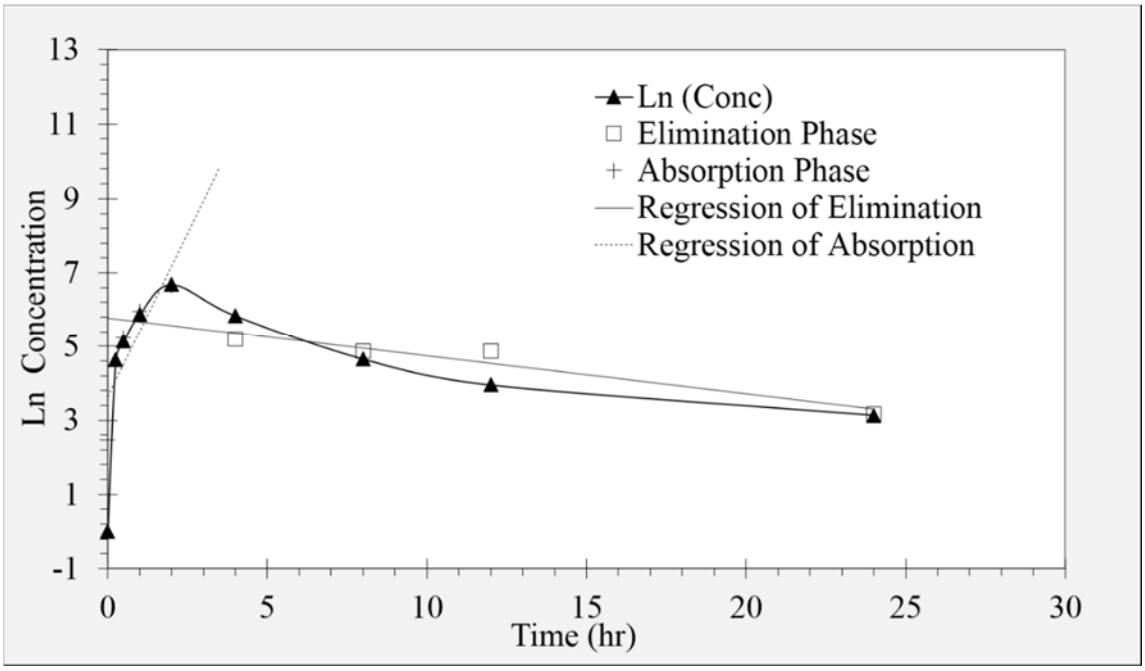

Figure 4.37 Ln concentration time profile including absorption and elimination phase for ACV:LT

Table 4.23 Pharmacokinetic Parameters of ACV after a single oral dose of ACV, in absence and presence of each of three different bioenhancers.

Parameter	Unit	Value			
		ACV	ACV:QU (5:2)	ACV:Sil (5:1)	ACV:LT (5:2.5)
Half Life (t1/2)	h	2.62	4.90	7.89	7.8
Time for maximum Concentration (Tmax)	h	1.5	2.0	2.0	2.0
Maximum Plasma Concentration (Cmax)	ng/ml	324	1026	890.33	798
Area under Curve AUC 0-t	ng/ml*h	1306.70	6347.02	4198.74	3554.12
AUC 0-inf_obs	ng/ml*h	2267.90	6660.47	4548.26	3813.45
Relative BA	%	1	4.85	3.71	2.71

4.3. Discussion

Low bioavailability of ACV presents a considerable challenge for the researcher from the very beginning. As, it is a very important and potent drug in herpes simplex virus therapy. In our proposed work, binary system of the ACV was prepared with three different bioenhancers using physical mixing method. Analytical method for the estimation of ACV was an important step for the whole research process, so for this purpose the most sophisticated and highly reliable instrument LC-MS was used. The results of LC-MS was very much reproducible and the method was properly validated before using for the samples. Uncertainty estimation further proofs the method reliability.

Ex-vivo studies were primary studies and were of important as they confirms the hypothesis behind the research work and encourages the team to go for further sophisticated and reliable technologies such as cell lines and *In-vivo* studies. The results of Ex-vivo studies revealed that the bioenhancers can plays a crucial role in the permeation enhancement of the ACV. The transport studies in caco-2 cell lines suggested that there is increase in the cellular uptake of ACV in the presence of the bioenhancers. The effective transport of the ACV in the presence of the bioenhancers most likely due to their P-gp inhibitory effect. The caco-2 cell lines also helps in optimization of the best ratios that can be used for the pharmacokinetic studies.

Pharmacokinetic studies were conducted in rabbits, these studies shows a significant increase in the plasma concentration of the ACV in the presence of the bioenhancers. It is well known fact that ACV is the substrate of the P-gp so it limits its oral uptake. As the bioenhancers used in the research work are P-gp inhibitor so the oral absorption has increased in the case of binary systems. In addition, to this it has also been reported that

the hepatic and intestinal first pass metabolism also effects on the bioavailability of the ACV. This east meets west technique, in combination with P-gp inhibition also helps in the metabolism as they also shown some effect of the CYP enzymes. So these bioenhancers may further advantage the bioavailability of ACV. The study of hepatic metabolism will be our future perspective. In Caco-2 cell lines the sequence of enhancement was higher of QU followed by the LT and Sil while in the in-vivo studies the pattern is QU followed by sil and then LT, as the in-vivo studies are more conclusive as they include the full pathways and all the factors hence the pharmacokinetic studies pattern can be used for the enhancement.

In this research work, ACV binary systems were prepared with the bioenhancrs to study their effect on the oral absorption. The studies carried out during this research work are compatibility studies, ex-vivo permeation studies, and transport across Caco-2 cell monolayers and pharmacokinetic studies. The results were promising showing significant changes in the permeation and transport across cell lines. Oral absorption also increases in the rabbits. The effect of the three bioenhacrers when compared QU shows the maximum enhancement following by the Sil and then by the LT. These promising results encourages us to focus on hepatic first pass metabolism bypass for further increase the absorption, these factors will be further needed to explore.

References

1. Fleming DT, McQuillan GM, Johnson RE, Nahmias AJ, Aral SO, Lee FK, et al. Herpes simplex virus type 2 in the United States, 1976 to 1994. N Engl J MED. 1997; 337(16):1105.
2. Kleymann G. Helicase primase: targeting the Achilles heel of herpes simplex viruses. Antiviral Chem Chemother. 2004;15 (3):135–40.
3. Fuertes, I., Miranda, A., Millan, M., Caraballo I. Estimation of the percolation thresholds in acyclovir hydrophilic matrix tablets. Eur. J. Pharm. Biopharm. 2006;64:336–342.
4. Jalonde, E. G., Blanco-Prieto, M. J., Ygartua, P., Santoyo, S. Increased efficacy of acyclovir loaded microparticles against herpes simplex virus type 1 in cell culture. Eur. J. Pharm. Biopharm. 2003;56:183–187.
5. Rossi, S. , Sandri, G. . Ferrari, F, M. C. Bonferoni, and C. Caramella. Buccal delivery of acyclovir from films based on chitosan and polyacrylic acid. Pharm. Dev. Technol. 2003;8:199–208.
6. Boon R. Antiviral treatment: from concept to reality. Antiviral Chem Chemother. 1997;8:5–10.
7. Darby G. A history of antiherpes research. Antiviral Chem Chemother. 1994;5:3–9.
8. International Conference on Harmonization, Q2B Validation of Analytical Procedures: Methodology, Consensus Guidelines, ICH Harmonized Tripartite Guidelines, 1996.
9. International Conference on Harmonization, Q2A Validation of Analytical Procedures: Consensus Guidelines, ICH Harmonized Tripartite Guidelines, 1994.

10. International organisation for standardization, ISO-IEC 17025:1999: General Requirements for the competence of Testing and Calibrating Laboratories, ISO, Geneva, 1999.
11. P. Hubert, J. Nguyen-Huu, B. Boulanger, et al. Harmonization of strategies for the validation of quantitative analytical procedures: A SFSTP proposal–Part III, J. Pharm. Biomed. Anal. 2007;45:82-96.
12. I. Hubatsch, E. G. E. Ragnarsson, P. Artursson. Determination of drug permeability and prediction of drug absorption in Caco-2 monolayers. Nature Protocols. 2007; 2(9):2111-2119.
13. R. Zhao, C. P. Hollis, H. Zhang, L. Sun, R. A. Gemeinhart, T. Li. Hybrid nanocrystals: achieving concurrent therapeutic and bioimaging functionalities toward solid tumors. Mol Pharm. 2011;8:1985–91.
14. D. R. Beriault, G. H. Werstuck. Detection and quantification of endoplasmic reticulum stress in living cells using the fluorescent compound, Thioflavin T. Biochim Biophys Acta. 2013; 1833:2293–301.
15. R. I. Freshney. Culture of animal cells: A manual of basic technique. New York: Wiley. 1987.